

Article

Muscle Fatigue Regulation through Muscle Activation Control in a Knee Hybrid Exoskeleton: Simulation Study

Shazan Ghajari ¹, Reihaneh Kardehi Moghaddam ^{1,*}, Hamidreza Kobravi ² and Naser Pariz ³ 

¹ Electrical Engineering Department, Mashhad Branch, Islamic Azad University, Mashhad P.O. Box 9187147578, Iran; ghajari.sh@alumni.um.ac.ir

² Research Center of Biomedical Engineering, Mashhad Branch, Islamic Azad University, Mashhad P.O. Box 9187147578, Iran; hamidrezakobravi@gmail.com

³ Department of Electrical Engineering, Faculty of Engineering, Ferdowsi University of Mashhad (FUM), Mashhad P.O. Box 9177948974, Iran; n-pariz@um.ac.ir

* Correspondence: r_k_moghaddam@mshdiau.ac.ir

Abstract: The knee hybrid exoskeleton is a system that aids in the rehabilitation of patients with mobility disorders. It comprises a powered exoskeleton and functional electrical stimulation, which moves the knee joint by stimulating the muscles. However, electrical stimulation of muscles can lead to muscle fatigue. For the first time, this article investigates the regulation of muscle fatigue by controlling muscle activation. To control muscle activation, an innovative adaptive controller for FES is designed. The adaptation law is designed utilizing a time-varying estimation of the muscle activation time parameter. The proportional-integral controller is designed to regulate the knee joint angle utilizing an electrical motor. The proportional-integral controller gains are calculated using an optimization method. A cooperative control structure is presented to use the electrical motor and functional electrical stimulation simultaneously. The muscle activation error is uniformly ultimately bounded, and its boundedness is proven through Lyapunov analysis; the error bound is also determined. The simulation results showed knee joint angle regulation and muscle fatigue regulation. The proposed control method results were compared with those based on model predictive control and switching control, which showed significant improvement in the joint angle error and muscle fatigue. The proposed method is appropriate for practical implementation based on the obtained results.

Keywords: adaptive control; hybrid exoskeleton; regulation problem; muscle fatigue; muscle activation; personalized rehabilitation



Citation: Ghajari, S.; Moghaddam, R.K.; Kobravi, H.; Pariz, N. Muscle Fatigue Regulation through Muscle Activation Control in a Knee Hybrid Exoskeleton: Simulation Study.

Machines **2023**, *11*, 937. <https://doi.org/10.3390/machines11100937>

Academic Editors: Rogério Sales Gonçalves and Giuseppe Carbone

Received: 2 August 2023

Revised: 31 August 2023

Accepted: 5 September 2023

Published: 1 October 2023



Copyright: © 2023 by the authors. Licensee MDPI, Basel, Switzerland. This article is an open access article distributed under the terms and conditions of the Creative Commons Attribution (CC BY) license (<https://creativecommons.org/licenses/by/4.0/>).

1. Introduction

Hybrid exoskeletons are rehabilitation tools for disorder movements and they are comprised of two main parts: (1) exoskeleton and (2) functional electrical stimulation (FES). The exoskeleton moves the joints mechanically using its actuators, which are motors. FES stimulates muscles with an electric current [1]—it sends current pulses to muscles and moves the joints by the stimulated muscles [2]. Although muscle electrical stimulation improves rehabilitation by stimulating the nervous system, it causes muscle fatigue and shortness of rehabilitation [3]. Hybrid exoskeletons can also be categorized in a general form, consisting of (1) multi-joint and single-joint lower limb hybrid exoskeletons and (2) multi-joint and single-joint upper limb hybrid exoskeletons [4]. One single-joint lower limb hybrid exoskeleton is the knee hybrid exoskeleton, which rehabilitates the knee joint [5]. The knee hybrid exoskeleton moves the knee joint towards the desired path or regulates it at the desired angle. In this paper, the knee hybrid exoskeleton is studied.

The automatic operation of hybrid exoskeletons is one of their essential features. Closed-loop controllers for electrical motors and FES play a central role in automating these devices [6]. The control objective of the hybrid exoskeletons is to solve the tracking or

regulation problem of joints. The most critical control challenge for these systems is the loss of system performance due to decreased actuators' efficiency, i.e., stimulated muscles, due to fatigue. The control of the knee hybrid exoskeletons is a research topic of interest; various studies have been conducted to control this device [7].

Switching control is one of the techniques employed to prevent the increase of fatigue in hybrid exoskeletons [8–14], wherein a class of switched systems is presented to describe switched hybrid exoskeletons [12]. In the design of the switching law for the lower limb hybrid exoskeletons, consideration is given to the threshold fatigue value, system stability, and attraction region of the controllers [9,11,12]. In [8,10], the fatigue region method is used for switching in the knee hybrid exoskeleton. In this method, two minimum and maximum threshold values for fatigue are defined. If the fatigue exceeds the maximum threshold, the switch will be made to the motor controller, and if the fatigue is below the minimum threshold, the switch will be made to the FES controller. The practical implementation constraints of the switching method are the possibility of chattering, delayed actuators, and physical limitations.

Hierarchical control is another method used to overcome the fatigue challenge [15–17]. In this method, a closed-loop control signal is calculated. Then, this signal is distributed between the motor and FES controllers by solving the optimization problem, one of the constraints of which is fatigue reduction. The computational complexity and the time-consuming nature of solving the optimization problem make implementing this method challenging. Determining the value of the local extremum instead of the global extremum can prevent muscle fatigue reduction by improper control distribution.

Model predictive controllers (MPCs) are used to regulate knee hybrid exoskeletons. These controllers use optimization methods to calculate the motor and FES control signals in a time frame [18–21]. One of the goals in the control signal distribution between the FES and the motor is to reduce muscle fatigue. Different MPCs regulate the knee hybrid exoskeleton, such as tube-based, penalty barrier function, and nonlinear MPC. In [19], a heuristic method is presented in the motor and FES control distribution to reduce muscle fatigue; however, in the results, a significant muscle fatigue increase is observed. In studies based on MPC methods, the muscle fatigue increase is significant [18,20,21].

Learning-based methods are used to estimate parameters or identify the model of hybrid exoskeletons. A learning-based controller is designed to overcome muscle fatigue [22]. A recurrent neural network, with supervised learning, identifies the system model, and a feedforward neural network, with a learning rule based on reinforcement learning, designs the controller. Neural network training requires a significant amount of data, which are not easily accessible. The training phase in learning-based methods may cause risks for the patient, and maintaining safety creates limitations in the learning process.

In some studies, the knee joint is controlled along with the hip joint or the ankle joint in cases where multi-joint exoskeletons of the lower limb are used for sitting–standing or walking. The sliding mode control has successfully controlled the joints, but the effect of the proposed method on muscle fatigue still needs to be investigated [23]. In [24], muscle synergies are used to control the hybrid exoskeleton. The complexity of muscle synergies calculation in practical implementation and the high dependence of this method on the system model are its disadvantages. A cooperative controller with a finite state machine is used to deal with fatigue [25–27]. The use of a finite state machine does not match the automation of the system. This method needs to be stronger for facing disturbance and environmental changes.

The studies used before to deal with muscle fatigue have some drawbacks: (1) In MPC-based methods, to face the muscle fatigue challenge, the control distribution between the motor and FES is achieved by solving the optimization problem, but the muscle fatigue increase in the obtained results is significant [18–21]. (2) In hierarchical control and MPC-based methods [15–21], which use optimization to prevent muscle fatigue increase, sub-optimal control values may be calculated at the boundary points instead of optimal values. In this way, reducing muscle fatigue is not optimal, and preventing the increase of

muscle fatigue is associated with errors. (3) In the reported results of hierarchical control methods, for people with spinal cord injury, the muscle does not respond to FES, the muscle fatigue is not calculated, and it is impossible to determine the FES control signal weight to decrease fatigue [15–17]. (4) In the methods based on switching, to compensate for muscle fatigue, FES is deactivated in specific time intervals; as a result, it becomes impossible to use the therapeutic benefits of electrical stimulation in those intervals [8–14]. (5) In addition, in switching-based methods, when FES is active, it is impossible to regulate muscle fatigue, and the amount of fatigue increases. (6) In learning-based methods, a large amount of data are needed to train the controllers. The controller is trained for simple movements, and it is not easy to access the training data set with various movement patterns [22]. In addition, the training stage is time-consuming and tiring for the patient. The disadvantages of the hybrid exoskeletons control methods, when dealing with muscle fatigue, include the optimization and learning challenges and the stimulation deactivation in switching. It is important to use a control method that prevents muscle fatigue increase by regulating it in a desired value, thus allowing the therapeutic advantages of FES usage without deactivating the electrical stimulation.

FES is important in hybrid exoskeletons. Electrical stimulation by stimulating the nervous system plays an influential role in the patient's sensory and motor rehabilitation. Electrical pulses stimulate sensory fibers, especially Ia fibers, that synapse with α -motoneurons in the spinal cord. In addition, motor neurons carry the electrical signal in the muscle and cause a muscle reflex. The release of calcium ions, Ca^{2+} , in muscle cells causes muscle recovery, and high-frequency electrical stimulation disrupts the calcium production in muscles and causes muscle fatigue [28]. In the proposed method of our study, it is possible to use sensory and motor stimulation of FES without increasing fatigue. Muscle fatigue regulation can prevent the need to stop the stimulation in rehabilitation.

Adaptive control is one of the effective methods for controlling hybrid exoskeletons [29]; due to the non-linear and time-varying nature of muscles, adaptive control is a suitable method for controlling FES [30]. In this article, the adaptive controller is used to control muscle activation. The muscle fatigue variable cannot be regulated directly with the control signal. Muscle activation is controllable through a control signal, and muscle fatigue is affected by the muscle activation variable; so, in this study, muscle activation control was used to regulate muscle fatigue. This study presents an innovative cooperative structure to control muscle activation and the knee joint's angle. In this structure, a proportional-integral (PI) controller controls the joint, whose gains are determined by the optimal control method. The proof of the uniformity ultimately boundedness (UUB) of the muscle activation error is done by the Lyapunov analysis method, which determines the bound of this error. The simulation of the proposed method is conducted on a model of a knee hybrid exoskeleton. The knee joint angle and the muscle activation are regulated to the desired references. Muscle fatigue is also regulated, and increased fatigue is prevented. The proposed method is compared with the model prediction control and switching control methods, which provides the best results in joint angle error and muscle fatigue value.

In Section 2, the description of the problem is presented. In this section, the dynamic models of the joint, muscle, and knee hybrid exoskeleton state space model are discussed. In Section 3, the presented method is elucidated. In this section, the design of joint and muscle activation controllers is presented, the mathematical correlation between the muscle activation and muscle fatigue is investigated, and the system stability is demonstrated through the utilization of a muscle activation controller. In Section 4, the simulation of the proposed method is conducted on a knee hybrid exoskeleton model, the results are analyzed, and the efficiency of proposed method is evaluated. In Section 5, the discussion is presented. In this section, the proposed method's performance, its advantages, and its clinical application privileges are discussed, and the limitations of the proposed method are pointed out. In Section 6, conclusions are made based on the previous sections, and future works are introduced.

2. Methods and Materials

The two primary actuators of the knee hybrid exoskeleton are the motor of the exoskeleton and the muscles stimulated by the electrodes connected to the FES; Figure 1 shows a picture of the knee hybrid exoskeleton and its actuators. To describe the system, equations that describe the dynamics of muscles and joints based on system inputs are needed [31]. The joint movement is caused by torque, the torque produced by the exoskeleton motor, and the torque produced by the electrical stimulation of the muscles.

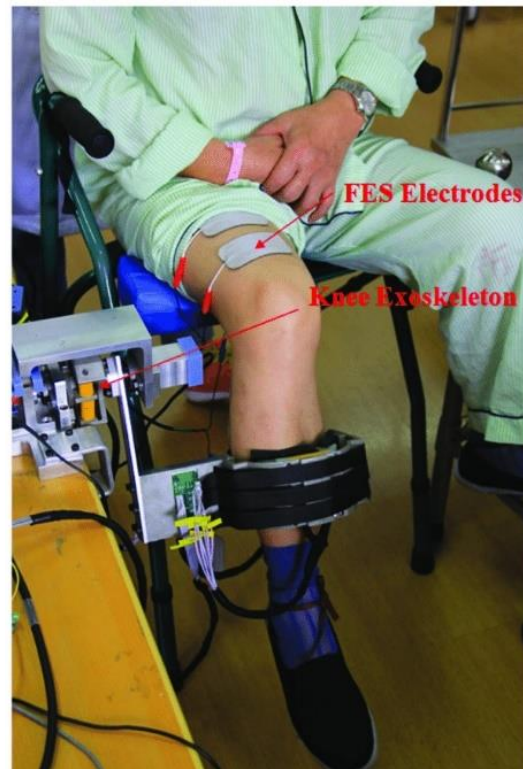


Figure 1. A picture of the knee hybrid exoskeleton [15].

Figure 2 shows a diagram of the knee hybrid exoskeleton, control signals, torques, and knee joint angles. FES sends an electrical current, $i(t) \in R^+$, through electrodes to the quadriceps muscles. As a result of stimulation, the muscles generate torque, $\tau_{ke} \in R$, and move the knee. The electrical motor produces mechanical torque, $\tau_m \in R$, in the knee and moves it. The joint moves with $\theta \in R$ angle, and the sensor transfers the $\theta(t)$ value to the controller, which is a computer or microcontroller. Based on the joint angle error, the controller calculates control signals for the motor, $u_m \in R$, and FES, $u_{ke} \in [0, 1]$. The controller sends these signals to the motor and FES to regulate the joint angle and muscle activation.

θ_{eq} is the knee equilibrium angle relative to the vertical axis [32]. Parameter, $\phi \in R$, is the knee anatomical angle and is calculated by Equation (1).

$$\phi = \frac{\pi}{2} - \theta - \theta_{eq} \quad (1)$$

In Figure 2, the center of mass of the shank, to which the mg force is applied, is specified; $m, g \in R^+$, are the mass of the shank and the acceleration gravity constant. $l_c \in R^+$, is the distance from the center of mass to the knee [32].

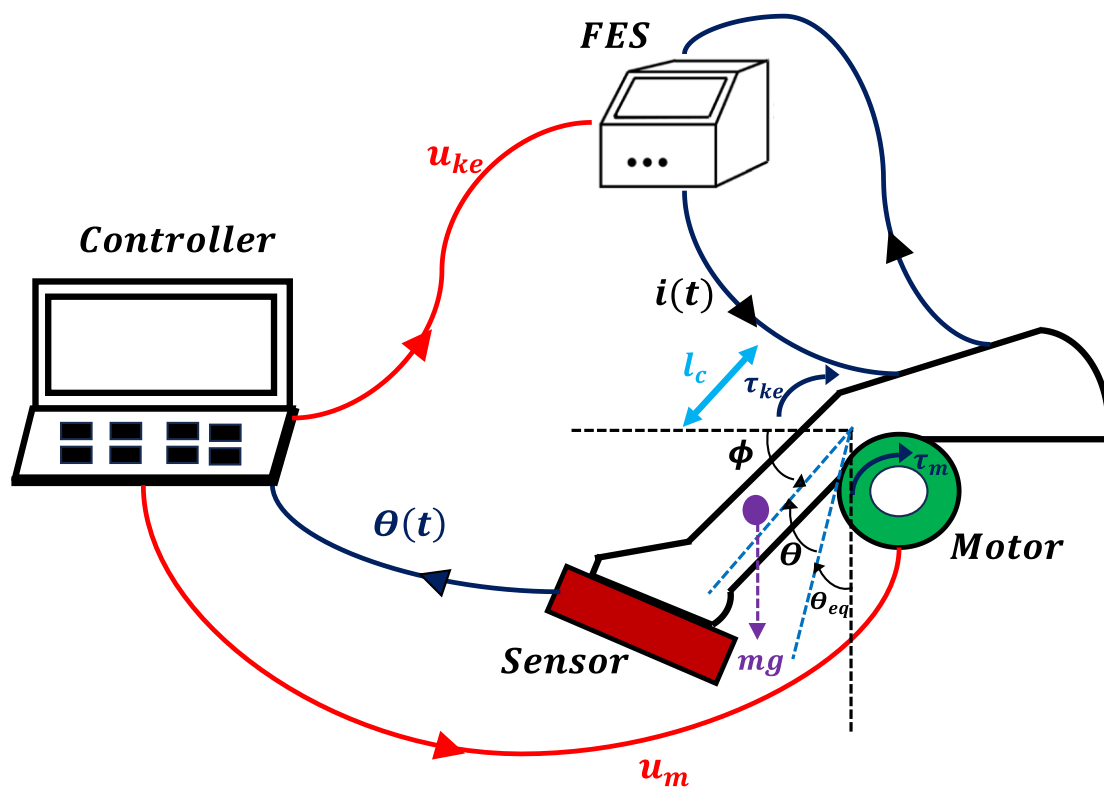


Figure 2. Schematic diagram of the knee hybrid exoskeleton.

2.1. Joint Dynamic Equation

The dynamic equation of the knee joint, according to Equation (2), is described by the Euler–Lagrange equation [33]. The equation’s inputs are the torques of the system, τ_m and τ_{ke} . The equation outputs are joint angle, θ ; angular velocity, $\dot{\theta} \in R$; and angular acceleration, $\ddot{\theta} \in R$. The constant parameter, $J \in R^+$, is the shank’s moment of inertia.

$$J\ddot{\theta} + G - \tau_p = \tau_{ke} + \tau_m \tag{2}$$

The torque created by applying gravity to the center of mass of the shank at the knee joint is the gravitational torque, $G(\theta)$. Equation (3) shows the expression of gravitational torque.

$$G(\theta) = mgl_c \sin(\theta + \theta_{eq}) \tag{3}$$

The passive dynamics of muscles, ligaments, and tendons create torque in the knee, which is called passive torque and is modeled by τ_p . Expression (4) shows passive torque; $\tau_p(\phi, \dot{\phi})$, is a function of the knee anatomical angle. The parameters $\phi_0 \in R$ and $d_i \in R$; $i \in \{1, 2, \dots, 6\}$ are patient-specific and model the stiffness and damping of the knee joint [32].

$$\tau_p = d_1(\phi - \phi_0) + d_2\dot{\phi} + d_3e^{d_4\phi} - d_5e^{d_6\phi} \tag{4}$$

The torque caused by the stimulated muscles, τ_{ke} , is expressed in Equation (5); this torque is created in the knee extension during electrical stimulation [31]. The term $c_2\phi^2 + c_1\phi + c_0$ is the torque length, and the term $1 + c_3\dot{\phi}(t)$ is the torque–velocity relationship. Parameters $c_j \in R$; $j \in \{0, \dots, 3\}$ are the patient-specific constants. The term α_{ke} is the muscle activation, and μ is the muscle fatigue obtained from the muscle dynamics equations.

$$\tau_{ke} = (c_2\phi^2 + c_1\phi + c_0) (1 + c_3\dot{\phi}) \alpha_{ke} \mu \tag{5}$$

2.2. Muscle Dynamic Equations

The dynamics of the stimulated muscle are described by two parameters of muscle activation and muscle fatigue [34,35]. The reason for the muscle stimulation is the electric current applied to it; Equation (6) expresses the electric current expression, $i(t) \in R^+$.

$$i(t) = I_t + u_{ke}(I_s - I_t) \quad (6)$$

$I_t \in R^+$ is the minimum current amplitudes that cause movement in the knee joint and $I_s \in R^+$ is the minimum current amplitude that causes maximum muscle contraction.

Dynamic of muscle activation, $\alpha_{ke} \in [0, 1]$, is expressed in Equation (7). The electrical stimulation control signal, u_{ke} , influences the dynamic of muscle activation. The parameter, $T_a \in R^+$, is the muscle activation time constant and is proportional to the duration of muscle stimulation.

$$\dot{\alpha}_{ke} = \frac{-\alpha_{ke} + u_{ke}}{T_a} \quad (7)$$

The muscle fatigue, $\mu \in [\mu_{min}, 1]$, dynamic is described by Equation (8). The expression, $(1 - \mu)(1 - \alpha_{ke})/T_r$, is the recovery term and the term, $(\mu_{min} - \mu)\alpha_{ke}/T_f$ is the fatigue term. The parameter, $T_r \in R^+$, is the recovery time constant, and parameter, $T_f \in R^+$, is the fatigue time constant.

$$\dot{\mu} = \frac{(\mu_{min} - \mu)\alpha_{ke}}{T_f} + \frac{(1 - \mu)(1 - \alpha_{ke})}{T_r} \quad (8)$$

The parameter $\mu_{min} \in (0, 1)$, determines the lower bound of muscle fatigue. $\mu = 1$, is equivalent to the non-fatigue state and $\mu = \mu_{min}$, is equivalent to maximum fatigue of the muscle.

2.3. State Space Equations

Joint and muscle dynamics describe the state space of the knee hybrid exoskeleton [31]. State space variables are, $x = [x_1, x_2, x_3, x_4]^T = [\theta, \dot{\theta}, \alpha_{ke}, \mu]^T$. The input signals are $u = [u_1, u_2]^T = [u_m, u_{ke}]^T$, which is $u_m = \tau_m$. To determine \dot{x}_2 , the expression (9) is written using Equation (2).

$$\ddot{\theta} = J^{-1}(\tau_{ke} + \tau_m - G + \tau_p) \quad (9)$$

By selecting $\dot{x}_2 = \ddot{\theta}$, the expression $\dot{x}_2 = J^{-1}(\tau_{ke} + u_1 - G + \tau_p)$ is obtained. The state space equations of the knee hybrid exoskeleton are written according to (10).

$$\dot{x} = f(x, u) = \begin{bmatrix} x_2 \\ \frac{1}{J}(u_1 + \tau_{ke} + \tau_p - G) \\ \frac{u_2 - x_3}{T_a} \\ \frac{(\mu_{min} - x_4)x_3}{T_f} + \frac{(1 - x_4)(1 - x_3)}{T_r} \end{bmatrix} \quad (10)$$

3. Proposed Control Method

In this study, an innovative cooperative structure is utilized for joint and muscle control. In the novel control structure, muscle activation is controlled separately from the joint angle and is accompanied by an independent reference signal. The adaptive controller regulates muscle activation, and the optimal PI controller regulates the joint angle. Figure 3 shows the block diagram of the controllers and the hybrid exoskeleton system.

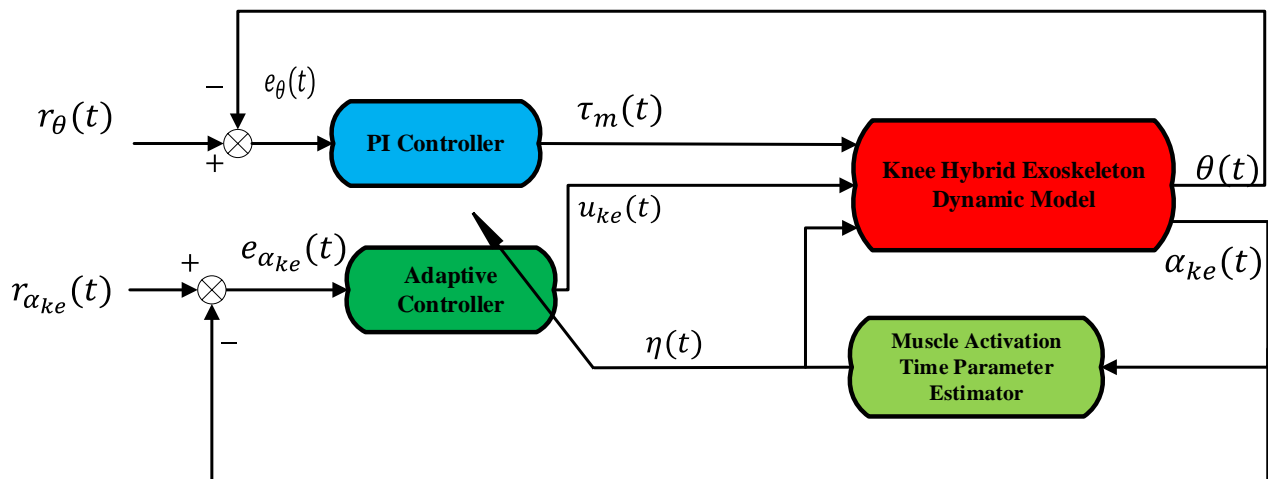


Figure 3. The block diagram of the controllers and hybrid exoskeleton system.

$r_{\alpha_{ke}}(t)$ is the reference signal for muscle activation and $r_{\theta}(t)$ is the the knee joint reference signal. $e_{\alpha_{ke}}(t) = r_{\alpha_{ke}}(t) - x_3(t)$ is the muscle activation error and $e_{\theta}(t) = r_{\theta}(t) - x_1(t)$ is the knee joint angle error. The controller design is based on model (10) of a knee hybrid exoskeleton. The muscle activation time parameter, $\eta(t)$, is estimated in the system model and used in the adaptive controller’s design.

3.1. Motor Control Signal

The motor control signal does not affect the stimulation torque, $\tau_{ke}(t)$, due to the separated design of the muscle activation controller. The stimulation torque acts as a disturbance in the dynamic of $x_2(t)$, so designing a robust controller for the knee joint is essential. The joint controller is an optimal PI controller [36]; PID-type controllers are suitable for tracking, are robust, and their gains calculation is not complex. The motor control signal, in the time interval $[0, t]$, is calculated by (11).

$$u_m(t) = k_p e_{\theta}(t) + k_I \int_0^t e_{\theta}(\tau) d\tau \tag{11}$$

Controller gains are $k_p, k_I \in R$; the optimization method calculates the controller gains according to (12).

$$k = [k_p \quad k_I]^T = \operatorname{argmin}_{k_p, k_I} \left(\int_0^t (e_{\theta}(\tau))^2 d\tau \right) \tag{12}$$

The term, $k = [k_p \quad k_I]^T$, is the vectro form of controller gains.

3.2. Muscle Controller

The adaptive control method is utilized to control the knee hybrid exoskeleton [37]. In this section, the adaptive controller is designed by an indirect adaptive control method to regulate muscle activation, thus regulating muscle fatigue. Lyapunov analysis, through the auxiliary variable method, proves the proposed method’s stability.

3.2.1. Muscle Fatigue Regulation

The dynamic of muscle fatigue is a function of muscle activation. Therefore, muscle fatigue is controlled by muscle activation. To regulate muscle fatigue, it is necessary that $\dot{\mu} = 0$; then, based on (8), Equation (13) is obtained.

$$\frac{(\mu_{min} - \mu)\alpha_{ke}}{T_f} = \frac{-(1 - \mu)(1 - \alpha_{ke})}{T_r} \tag{13}$$

By multiplying both sides of (13) by $T_f T_r$, the expression $T_r \mu_{min} \alpha_{ke} - T_r \mu \alpha_{ke} = -T_f + T_f(\mu + \alpha_{ke}) - T_f \mu \alpha_{ke}$, is obtained. By arranging sentences and factoring common terms, α_{ke} , can be determined in terms of μ , according to (14).

$$\alpha_{ke} = \frac{-T_f + T_f \mu}{T_r \mu_{min} - T_f + (T_f - T_r) \mu} \quad (14)$$

By placing the desired value of μ in (14), the value at which the muscle activation by u_2 should be regulated is obtained. Relation (15) shows the expression of muscle fatigue in terms of muscle activation. With this relationship, it is possible to obtain the amount of fatigue according to each muscle activation regulated value.

$$\mu = \frac{(T_f - T_r \mu_{min}) \alpha_{ke} - T_f}{(T_f - T_r) \alpha_{ke} - T_f} \quad (15)$$

3.2.2. Estimation of Muscle Activation Time Parameter

In the design of the FES controller, the indirect adaptive control method is used, so a parameter in the system dynamic is estimated, and this parameter is utilized in the controller design. In the dynamic equation of muscle activation, the only constant parameter is the inverse of muscle activation time constant. So, parameter $1/T_a$, is estimated to design the FES controller.

The dynamic equation of, $x_3(t)$, is written as (16)

$$\dot{x}_3(t) = \frac{u_2(t) - x_3(t)}{T_a} = \frac{u_2(t)}{T_a} - \frac{x_3(t)}{T_a} \quad (16)$$

The change of variable, $u_2 = u_2/T_a$, is applied in (16) to prevent complexity in the state equation expression. Equation (17) is derived as follows:

$$\dot{x}_3(t) = u_2(t) - \frac{x_3(t)}{T_a} \quad (17)$$

where $1/T_a$, is replaced by the time varying parameter, $\eta(t)$, and the state space equations is rewritten as (18).

$$\dot{x} = f(x, u) = \begin{bmatrix} x_2 \\ \frac{1}{J}(u_1 + \tau_{ke} + \tau_p - G) \\ u_2 - \eta x_3 \\ \frac{(\mu_{min} - x_4)x_3}{T_f} + \frac{(1-x_4)(1-x_3)}{T_r} \end{bmatrix} \quad (18)$$

The $\eta(t)$ is estimated by (19); $\gamma \in R$ is a constant [30].

$$\dot{\eta}(t) = -\gamma x_3(t) e_{\alpha_{ke}}(t) \quad (19)$$

3.2.3. FES Control Signal

The adaptive control signal, $u_{ke}(t)$, is expressed in (20) [38–40]. The control signal comprises the state feedback, $\eta(t)x_3(t)$, and a proportional term, $\kappa e_{\alpha_{ke}}(t)$ [41]. By applying the term $\eta(t)x_3(t)$, the adaptation parameter is involved in the control signal.

$$u_{ke}(t) = \kappa e_{\alpha_{ke}}(t) - \eta(t)x_3(t) \quad (20)$$

The term $\kappa e_{\alpha_{ke}}(t)$ is used to compensate for the muscle activation tracking error; $\kappa \in R^+$, is a constant parameter. The controller adaptation law is the Equation (19). Figure 4 shows the block diagram of the joint and muscle controllers and their state equations.

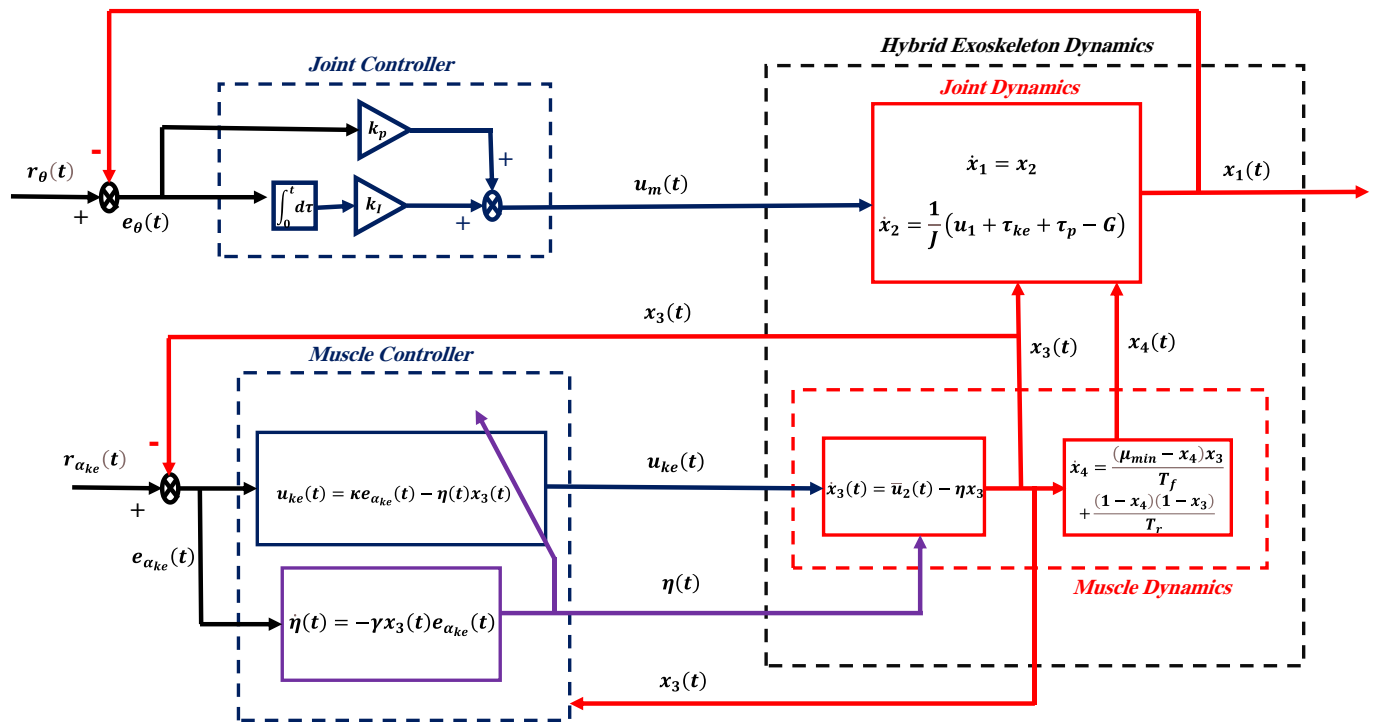


Figure 4. Joint and muscle controllers and state equations.

3.2.4. Stability Analysis

Because $\eta(t)$ is unknown, the approximated term $\hat{\eta}(t)$ is considered for the muscle activation time coefficient, and the estimation error is calculated by $\tilde{\eta}(t) = \hat{\eta}(t) - \eta_d$, where η_d is the desired value of the muscle activation time coefficient.

Assumption 1. According to the physical characteristics of the knee hybrid exoskeleton system, the estimation error $\tilde{\eta}$ is bounded as $|\tilde{\eta}| < \Delta_\eta$ [42].

Theorem 1. The hybrid exoskeleton system is considered with the dynamic Equation (18) and the control signal with Equations (19) and (20). If $\kappa \in R^+$ and $\gamma \in R$ are such that $(1/2)\gamma^2 - \kappa + 1 < 0$, then the muscle activation error is uniformly ultimately bounded.

Proof. Define the Lyapunov function $V(\tilde{\eta}, e_{\alpha_{ke}}) = (1/2)\tilde{\eta}^2 + (1/2)e_{\alpha_{ke}}^2$ and consider the auxiliary variable $Z = [\hat{\eta}(t) \quad e_{\alpha_{ke}}(t)]$ and determine the boundary (21) for the Lyapunov function. In (21), $\lambda_1, \lambda_2 \in R^+$ and $\lambda_1 < \lambda_2$ is considered.

$$\lambda_1 \|Z\|^2 \leq V \leq \lambda_2 \|Z\|^2 \tag{21}$$

Taking a derivative from $V(\tilde{\eta}, e_{\alpha_{ke}})$, the expression $\dot{V}(\tilde{\eta}, e_{\alpha_{ke}}) = \dot{\tilde{\eta}}\tilde{\eta} + \dot{e}_{\alpha_{ke}}e_{\alpha_{ke}}$, is obtained. According to the relationship $e_{\alpha_{ke}}$, and considering that the desired value $r_{\alpha_{ke}}$ is a constant value, and $\dot{e}_{\alpha_{ke}} = -\dot{x}_3$. Replacing the expression (19) and the expression \dot{x}_3 from (18) in \dot{V} , (22) is obtained.

$$\dot{V} = (-\gamma x_3 e_{\alpha_{ke}})\tilde{\eta} - (u_2 - \hat{\eta}x_3)e_{\alpha_{ke}} \tag{22}$$

As $\bar{u}_2 = u_{ke}$, (20) is replaced in (22), expression (23) is obtained.

$$\dot{V} = -\gamma x_3 e_{\alpha_{ke}}\tilde{\eta} + 2\hat{\eta}x_3 e_{\alpha_{ke}} - \kappa e_{\alpha_{ke}}^2 \tag{23}$$

According to Assumption 1 and considering $x_3 = \alpha_{ke} \in [0, 1]$, using Young's inequality, inequalities (24) can be written.

$$\begin{aligned} -\gamma x_3 e_{\alpha_{ke}} \tilde{\eta} &\leq \frac{1}{2} \gamma^2 e_{\alpha_{ke}}^2 + \frac{1}{2} \Delta_{\eta}^2 \\ 2\hat{\eta} x_3 e_{\alpha_{ke}} &\leq \hat{\eta}^2 + e_{\alpha_{ke}}^2 \end{aligned} \quad (24)$$

Using (24), inequality (25) can be written for the expression (23).

$$\dot{V} \leq \left(\frac{1}{2} \gamma^2 - \kappa + 1\right) e_{\alpha_{ke}}^2 + \hat{\eta}^2 + \frac{1}{2} \Delta_{\eta}^2 \quad (25)$$

The expression, $(\frac{1}{2} \gamma^2 - \kappa + 1) e_{\alpha_{ke}}^2 + \hat{\eta}^2$ is replaced on the right side of inequality (25) by $\min\left\{1, \frac{1}{2} \gamma^2 - \kappa + 1\right\} \|Z\|^2$. According to the assumption of Theorem 1, $\min\left\{1, \frac{1}{2} \gamma^2 - \kappa + 1\right\} \|Z\|^2 = -\left(\frac{-1}{2} \gamma^2 + \kappa - 1\right) \|Z\|^2 = -K \|Z\|^2$ can be written, which is $K > 0$. Inequality (25) can be written as (26).

$$\dot{V} \leq -K \|Z\|^2 + \frac{1}{2} \Delta_{\eta}^2 \quad (26)$$

The expression K/λ_2 is added and subtracted on the right side of (26); based on (21), inequality (26) can be written as (27).

$$\dot{V} \leq -\frac{K}{\lambda_2} V - \frac{K}{\lambda_2} + \frac{1}{2} \Delta_{\eta}^2 \quad (27)$$

The expression, $\frac{-K}{\lambda_2} + \frac{1}{2} \Delta_{\eta}^2$, is replaced with Δ' , the sides of (27) is multiplied by $e^{\frac{-K}{\lambda_2} t}$, and by taking the integral, (28) is obtained.

$$V \leq V_0 e^{\frac{-K}{\lambda_2} t} + \frac{\lambda_2}{K} \Delta' \left(1 - e^{\frac{-K}{\lambda_2} t}\right) \quad (28)$$

Using (28) and based on (21), inequality (29) can be written.

$$\|Z\| \leq \sqrt{\frac{\lambda_2}{\lambda_1} \left(\|Z(0)\|^2 - \frac{\Delta'}{K}\right) e^{\frac{-K}{\lambda_2} t} + \sqrt{\frac{\lambda_2}{\lambda_1} \Delta'}} \quad (29)$$

According to (29), $\|Z\|$ is ultimately uniformly bounded, so the muscle activation error signal $e_{\alpha_{ke}}$, which constitutes $\|Z\|$, is also ultimately uniformly bounded [19]. \square

4. Simulation Results

The simulation was performed in a MATLAB environment and the sampling frequency was set to $\nu = 100$ Hz [20,32]. The simulation time was set to $T = 120$ s. The adaptive controller parameters were set as $\kappa = 1$ and $\gamma = 0.2$, and the PI controller gains were calculated as $k_p = 92.95$ and $k_I = 119.27$. The desired simulation had two main goals: (1) regulation of knee joint angle and (2) regulation of muscle activation. Achievement of muscle activation regulation is the control of muscle fatigue. Table 1 shows the system dynamic equations parameters.

In the following section, the controllers' performance is evaluated, then the performance of the proposed method is compared with the other knee hybrid exoskeleton controlling methods.

Table 1. The parameters of system dynamic equations.

Parameter	Value	Parameter	Value	Parameter	Value	Parameter	Value
I_t [mA]	18.1	d_1	2.66×10^{-14}	ϕ_0 [rad]	5.29×10^{-8}	T_r [s]	48.09
I_s [mA]	60	d_2	1.68	c_0	78.78	T_a [s]	0.26
M [kg]	4.69	d_3	1.64	c_1	55.76	T_f [s]	29.17
l_c [m]	37	d_4	1.59	c_2	-49.02		
J [kg/m]	0.19	d_5	0.76	c_3	1.44		
θ_{eq} [rad]	1.2	d_6	-39.09	μ_{min}	2.61×10^{-9}		

4.1. Assessment of Controllers Performance

In the performance assessment of controllers in hybrid exoskeletons, the results of the system in the tracking of references; the value of inputs, i.e., control signals and torques; and the amount of muscle fatigue are investigated. First, to evaluate the controller's performance in regulation, the main control objective of the hybrid exoskeleton is checked; if the controller regulates the system appropriately, measuring the muscle fatigue becomes important. In case of inappropriate regulation error, the controller needs to be modified. In addition, this section evaluates the control structure performance in joint and muscle control using multi-level angle and activation references.

To avoid sudden movements of the knee joint, reference signals increase gradually from the initial value to the steady value; this movement limitation is considered in the simulation. Equation (30) expresses a knee joint reference signal.

$$r_{\theta}(t) = \begin{cases} 6t; 0 \leq t \leq 10 \\ 60; 10 < t \leq 120 \end{cases} \quad (30)$$

Muscle activation reference is considered in (31). Simulations are repeated for three values of $\alpha_{ke,ref} = \{0.07, 0.2, 0.5\}$.

$$r_{\alpha_{ke}}(t) = \begin{cases} \left(\frac{\alpha_{ke,ref}}{10}\right)t; 0 \leq t \leq 10 \\ \alpha_{ke,ref}; 10 < t \leq 120 \end{cases} \quad (31)$$

4.1.1. Regulation Results

This section investigates the results of knee joint regulation, muscle activation regulation, and their errors. Figure 5 shows the results of knee joint regulation and knee joint angle error.

The knee joint is regulated in the muscle activation references by the proposed control method. The joint controller regulates the knee with an acceptable error. The overshoot is observed when starting the steady state of the angle reference. As the reference value of muscle activation increases, the overshoot also increases.

The torque caused by FES, τ_{ke} , acts as a disturbance for the knee joint. With the increase in the muscle activation value, the stimulation torque also increases, and as a result, the overshoot increases. The PI controller is robust to the disturbance caused by stimulation torque and regulates the knee joint successfully as a result.

Figure 6 shows the muscle activation regulation results. In muscle activation regulation, by increasing the reference value, an overshoot in muscle activation occurs, such as an overshoot in angle. The muscle activation is regulated agreeably.

The reason for the overshoot can be explained by the activation controller adaptation. As the activation reference value increases, the initial activation error increases. Because the adaptation parameter is a function of the error, the adaptation parameter value increases. As a result, the activation control signal increases, and this increase appears as an overshoot in muscle activation.

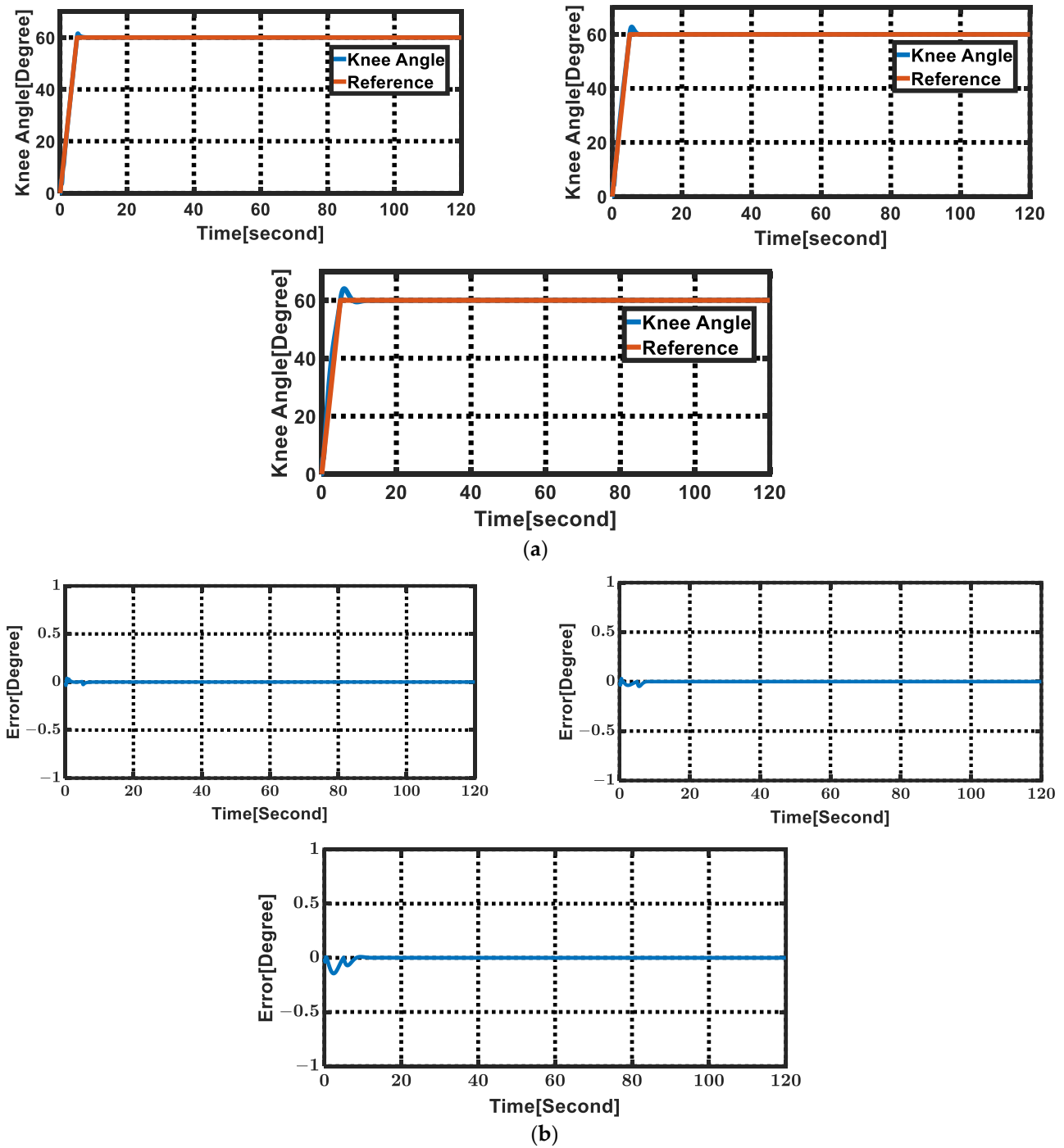


Figure 5. (a) Knee angle regulation and (b) knee angle error. From up left to right and down for $r_{\alpha_{ke}} = \{0.07, 0.2, 0.5\}$.

Table 2 shows the performance results of the proposed method for different muscle activation references. The maximum amplitude of the electrical current, the steady electrical current amplitude, the RMS error of angle, and the overshoot are presented in Table 3. The RMS error of the knee joint angle, $e_{\theta,RMS}$, in the time interval $[t_0, t_f]$, is calculated using (32).

$$e_{\theta,RMS} = \sqrt{\frac{1}{(t_f - t_0)} \int_{t_0}^{t_f} e_{\theta}(\tau) d\tau} \quad (32)$$

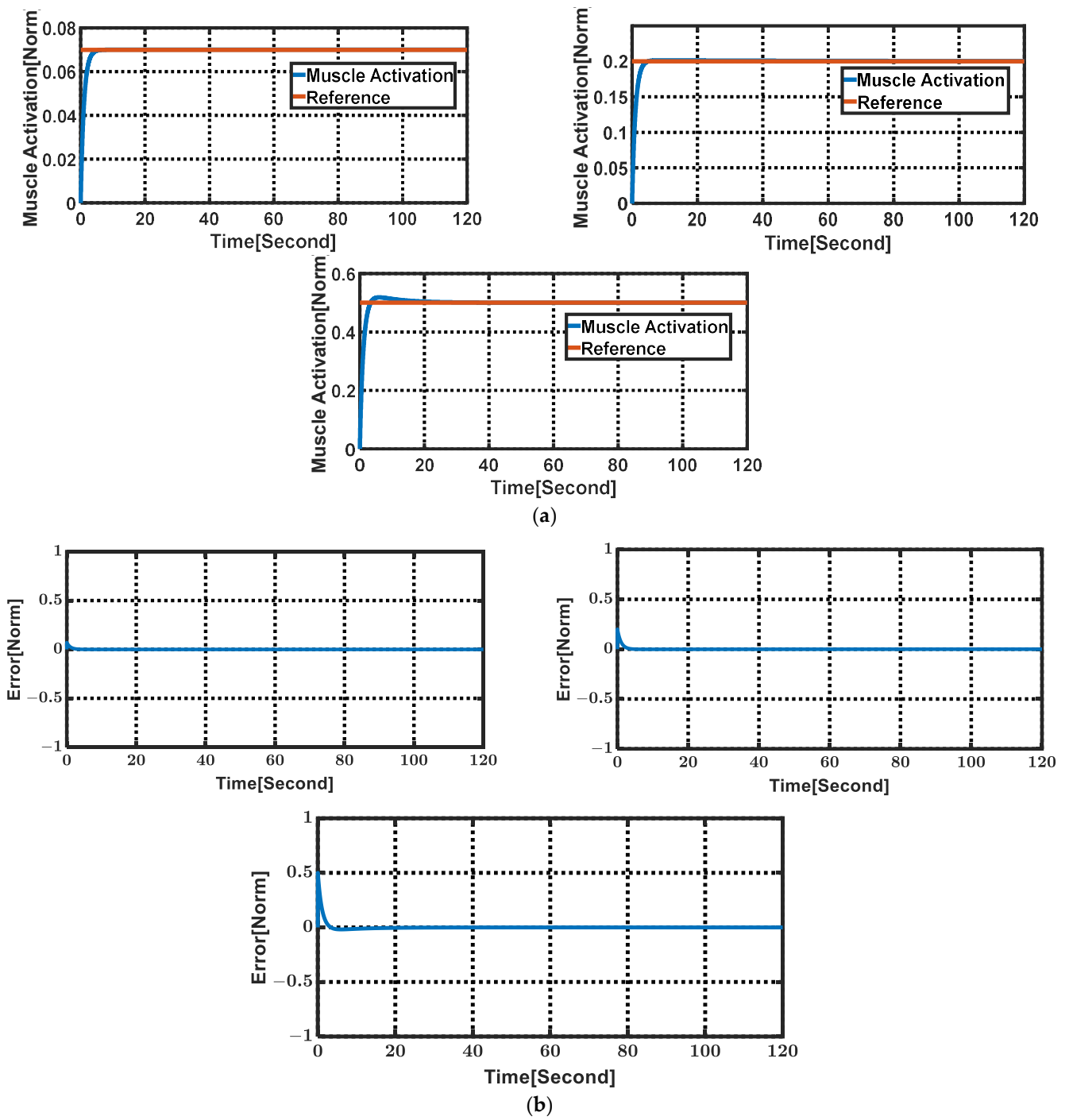


Figure 6. (a) Muscle activation regulation and (b) muscle activation error. From top left to right and below for $r_{\alpha_{ke}} = \{0.07, 0.2, 0.5\}$.

Table 2. Performance results for the proposed method.

$r_{\alpha_{ke}}$	Maximum Current [mA]	Current Steady Value [mA]	RMS Error [Degree]	Overshoot [Degree]
0.07	29.67	25.99	0.17	1.51
0.2	36.49	25.99	0.36	2.73
0.5	52.50	26	1.14	3.99

Table 3. Muscle fatigue converged values.

α_{ke} Converged Value	Muscle Fatigue Converged Value
0.07	0.84
0.2	0.62
0.5	0.29

4.1.2. Control Signals and Torques

The torques are system inputs, and an evaluation of their performance is essential because if the control objectives are achieved, in the simulation, with values incompatible with the physical constraints, the controller does not have practical efficiency. Because torques are determined based on control signals, it is necessary to assess the control signals.

Figure 7 shows the motor control signal for the muscle activation references; the motor torque is the same as the motor control signal. As shown in Figure 7, the motor torque is converged at a constant value by regulation of the knee angle.

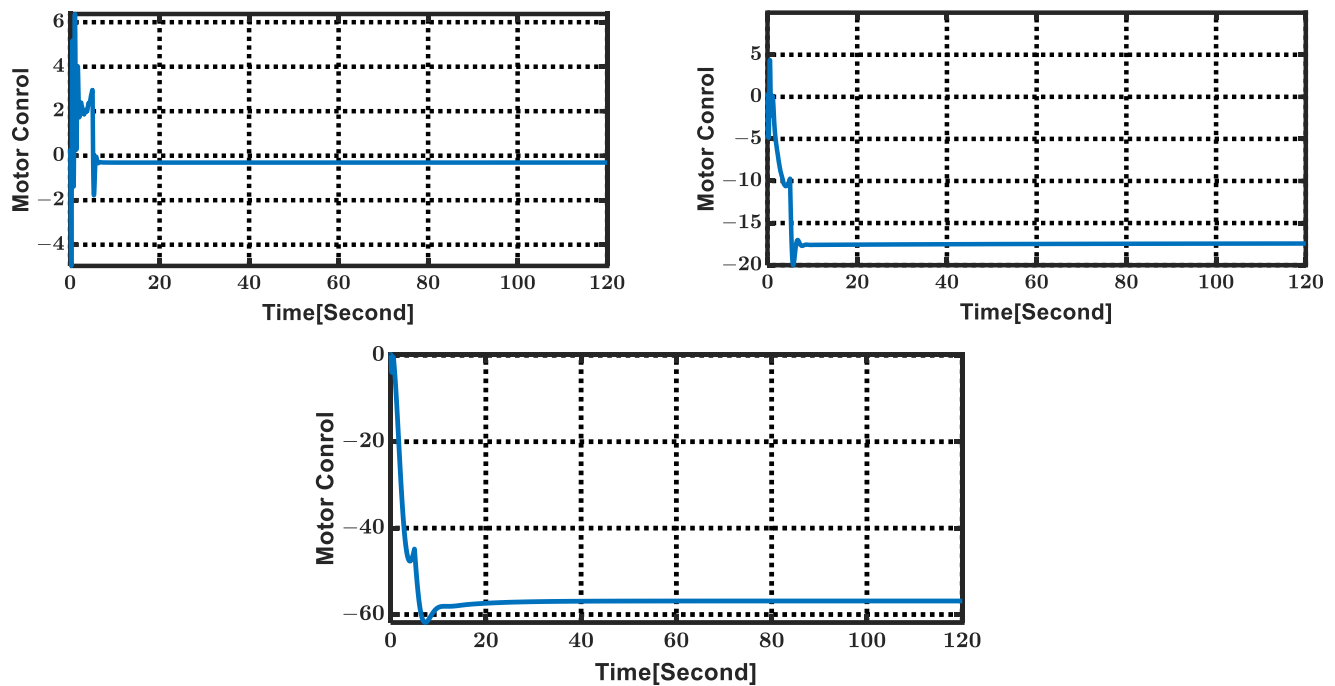


Figure 7. Motor control signals from top left to right and below for $r_{\alpha_{ke}} = \{0.07, 0.2, 0.5\}$.

By increasing the muscle activation reference, the absolute value of the motor torque converged in a more significant value. As the stimulation torque increased, according to \dot{x}_2 equation, a larger $|\tau_m|$ was needed to counteract it. Therefore, by increasing the activation reference, $|\tau_m|$ also increased.

Figure 8 shows FES control and adaptation parameter signals for different activation muscle references. The muscle activation time parameter changed according to the variations of the muscle activation error, and when the error signal was converged, the time parameter also converged to a constant value.

The FES control signal was reduced to zero by the convergence of the muscle activation error, which is proportional to the adaptiveness of the controller. By regulating the muscle activation, there is no need to calculate the stimulation control signal, thus avoiding unnecessary calculations for the controller.

Figure 9 shows the FES torque; the stimulation torque converged to a fixed value by converging the control signal. The amount of torque produced was sufficient to regulate muscle activation.

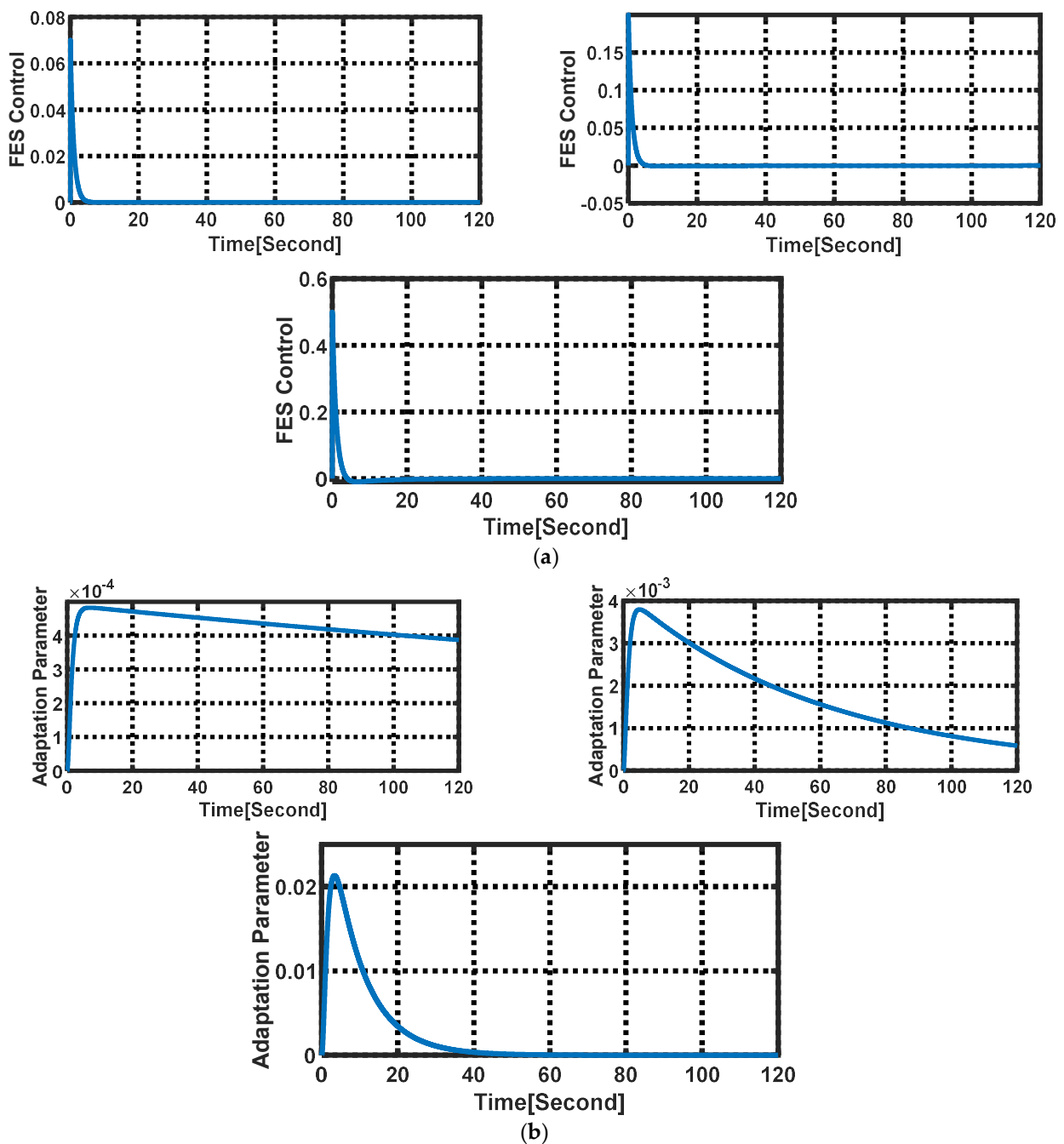


Figure 8. (a) Functional electrical stimulation (FES) control signals and (b) adaptation parameters. From up left to right and down for $r_{\alpha_{ke}} = \{0.07, 0.2, 0.5\}$.

The stimulation torque is in an acceptable range; with an increase in muscle activation reference value, more significant torque was produced to regulate the activation. The adaptive control method for the muscle prevented the production of excess torque, which could cause fatigue after regulating the muscle activation.

4.1.3. Assessment of Muscle Fatigue Regulation

The proposed method's performance in muscle fatigue regulation was evaluated using three desired muscle fatigue values, $\mu_d \in \{0.2, 0.6, 0.8\}$, and their corresponding muscle activations according to (14). The pairs, $(\mu_d, \alpha_{ke}) \in \{(0.2, 0.5), (0.6, 0.2), (0.8, 0.07)\}$, were the values of desired muscle fatigues and their corresponding regulated muscle

activations. Control signals generated in 4.1.2 regulated muscle activation; Figure 10 shows the simulation results for muscle fatigue.

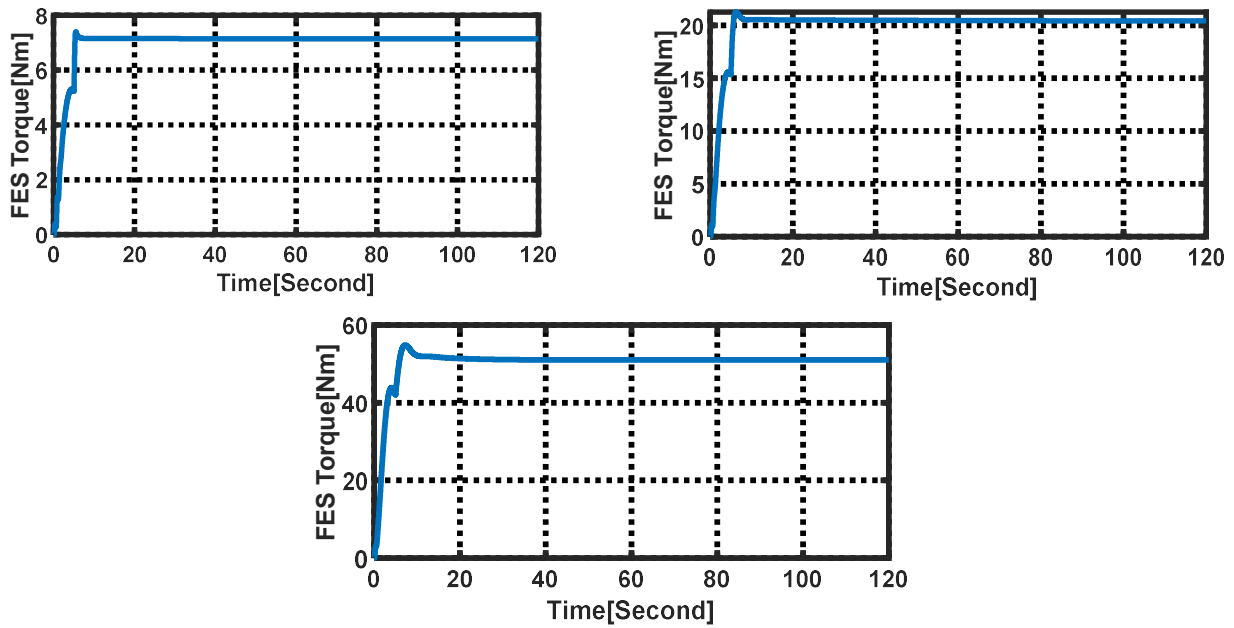


Figure 9. FES torques. From up left to right and down for $r_{\alpha_{kc}} = \{0.07, 0.2, 0.5\}$.

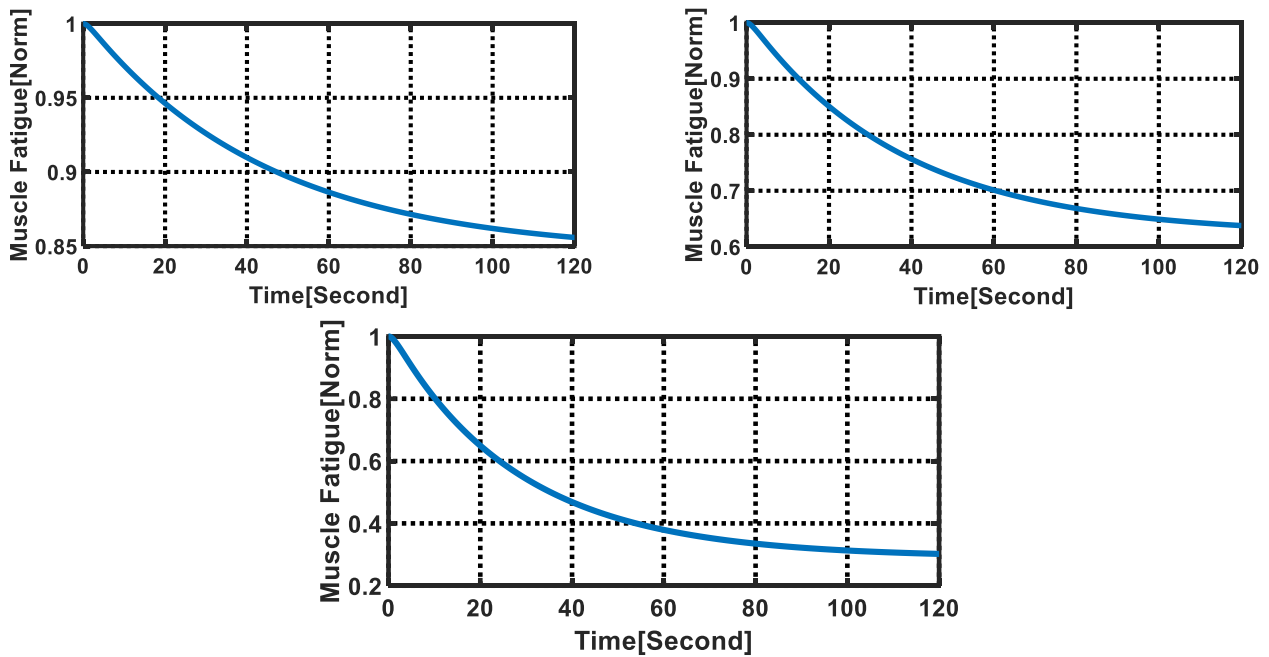


Figure 10. Muscle fatigue results. From top left to right and down for $r_{\alpha_{kc}} = \{0.07, 0.2, 0.5\}$.

Muscle fatigue values are successfully regulated to the desired values. Table 3 shows the regulated values of muscle fatigue and muscle activation based on simulation results.

To check the convergence of muscle fatigue values, its phase portrait is plotted in the $\mu - \dot{\mu}$ plane [38]. Figure 11 shows the phase portrait of muscle fatigue.

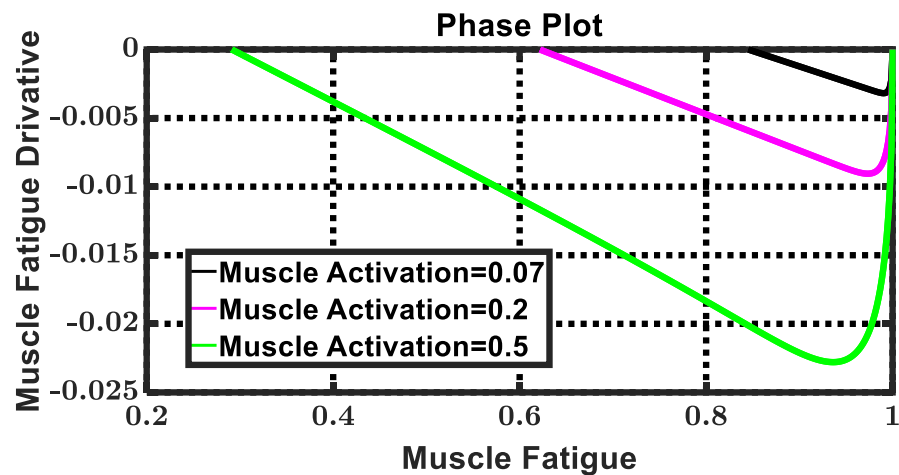


Figure 11. Phase plot of muscle fatigue.

For each of the three desired values of muscle fatigue, the simulation started from the initial value of $(\mu_0, \dot{\mu}_0) = (1, 0)$. The values of muscle fatigue and its derivative, after going through the phase curve, in values $(\mu_f, \dot{\mu}_f) \in \{(0.2, 0), (0.6, 0), (0.8, 0)\}$, converged. Zero values of $\dot{\mu}_f$ indicated the regulation of muscle fatigue, and μ_f values indicated the fatigue regulation in the desired values.

4.1.4. Assessment of Control Structure Performance

The coupling of controllers is considered an undesirable phenomenon. To evaluate the coupling of the muscle controller and joint controller, a simulation was conducted for multi-level references of muscles and joints. Multiple references were used for angle reference in [32,43]. Relation (33) shows the multiple angle reference.

$$r_\theta(t) = \begin{cases} 4.5t; 0 \leq t < 10 \\ 45; 10 < t \leq 30 \\ 1.5t; 30 < t \leq 40 \\ 60; 40 < t \leq 60 \\ 2t - 60; 60 < t \leq 70 \\ 80; 70 < t \leq 120 \end{cases} \quad (33)$$

The multiple muscle activation reference is shown by (34).

$$r_{\alpha_{ke}}(t) = \begin{cases} 0.02t; 0 \leq t < 10 \\ 0.2; 10 \leq t < 40 \\ 0.02t - 0.6; 40 \leq t < 50 \\ 0.4; 50 \leq t \leq 120 \end{cases} \quad (34)$$

Figure 12 shows the results of the knee joint angle and muscle activation regulation. The proposed method can regulate knee joint angle in multiple references, with multiple muscle activations.

The muscle and joint controller successfully followed multi-level references, and their performance was not coupled. Therefore, the proposed structure was suitable for controlling the knee hybrid exoskeleton.

The required FES current for multiple knee joint angle references and multiple muscle activation references is shown in Figure 13.

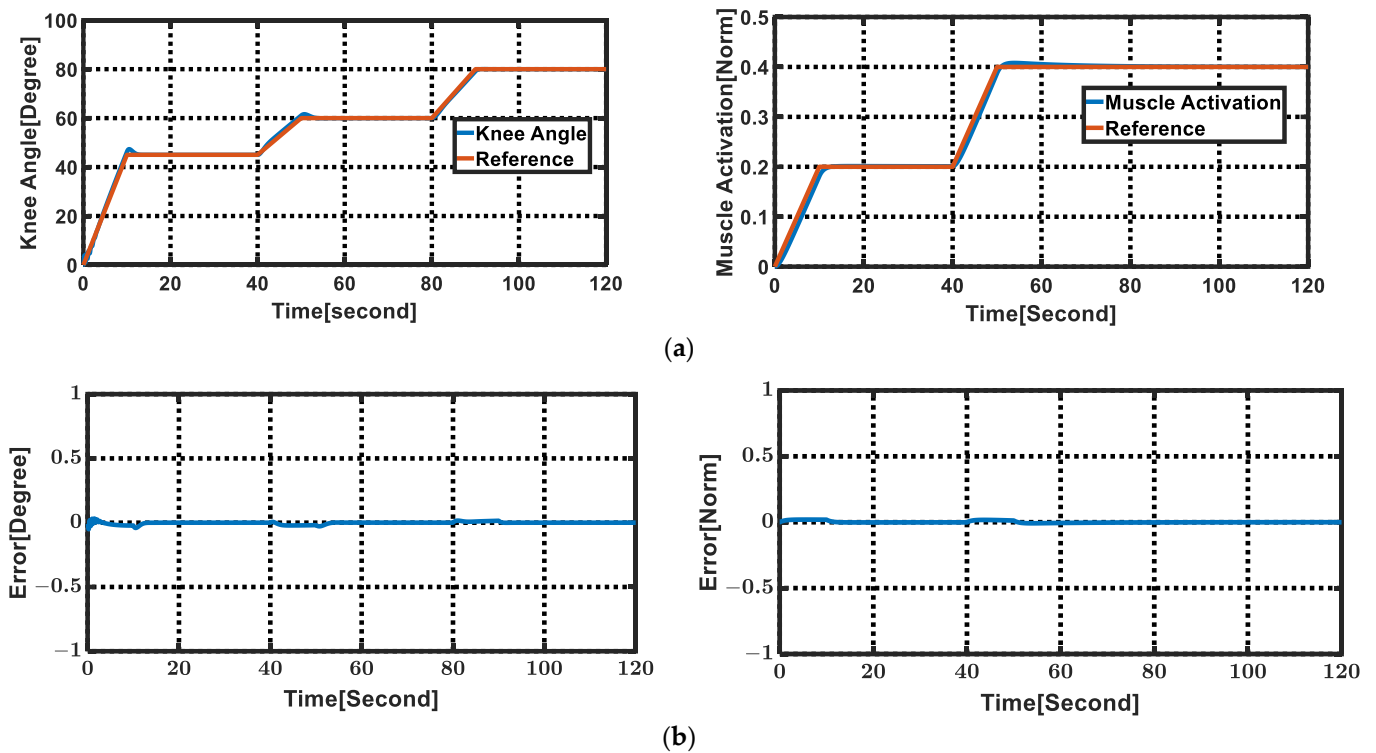


Figure 12. (a) Knee joint angle and muscle activation (left to right) and (b) knee joint angle error and muscle activation error (left to right).

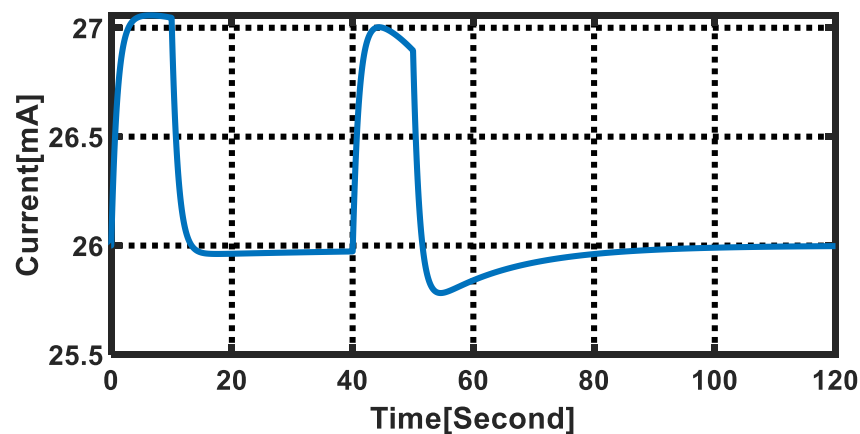


Figure 13. FES current for multiple references.

The current required for the stimulation was produced in an acceptable range, and it was possible to implement multi-level regulation.

4.2. Comparison with Other Methods

In this section, to evaluate the proposed method compared with the other control methods, this method was compared with methods based on model predictive control and switching control for the knee hybrid exoskeleton. Model predictive control has been used many times in previous works to control the knee hybrid exoskeleton. Switching control has also been used to deal with fatigue in controlling hybrid exoskeletons. Several indexes have been considered in the evaluations, but the results of regulation and the amount of fatigue were of priority for evaluation.

4.2.1. Comparison with MPC Methods

MPC-based methods are used to control the knee hybrid neuroprosthesis; in the studies conducted using the MPC method, the current amplitude of the electrical stimulation was investigated [32]. In this section, the proposed method was compared with the nonlinear model predictive control (NMPC) method in the current amplitude. In addition, the muscle fatigue caused by the proposed method was compared with that caused by tube-based NMPC and feedback-linearized NMPC methods.

Table 4 shows the electrical current values for the proposed method and NMPC method. The average current in the last 10 s of simulation and the maximum current resulting from the proposed method were 48.72% and 52.63%, respectively, lower than the similar indexes achieved by the NMPC [19].

Table 4. Current values.

Controller	Average Current [mA]	Maximum Current [mA]
Proposed Method	20	26
NMPC	38	55

Stimulation current is the main reason for increasing the muscle fatigue in hybrid exoskeletons. The production of less current by the proposed method led to less muscle fatigue than the NMPC method.

Table 5 shows the minimum muscle fatigue results from the proposed method, the tube-based NMPC, and the feedback-linearized NMPC [20,21]. The results showed a 60% reduction compared with the tube-based NMPC and a 20% reduction compared with the feedback-linearized NMPC.

Table 5. Minimum muscle fatigue.

Controller	Minimum Muscle Fatigue
Proposed Method	0.8
Tube based NMPC	0.4
Feedback linearized NMPC	0.7

4.2.2. Comparison with Switching Methods

The proposed method in knee joint regulation and muscle fatigue control was compared with the simulations performed with the variable gain super twisting sliding mode control (VGSTSMC) switching method and hybrid PID switching method to assess the performance of this method [8,14]. In [8], fatigue region switching, and in [14], persistent dwell time (PDT) switching, were the methods to prevent the increase in muscle fatigue. In [8], the VGSTSM controller was used for motor and FES control, and in [14], two optimal PID controllers were used for motor and FES. The knee hybrid exoskeleton was the main plant for both methods. Table 6 shows the gains of PID controllers in the hybrid PID method.

Table 6. Controller parameters in the hybrid PID method.

Controller	k_I	k_d	k_p
Motor	0.65	0.92	1.87
FES	454.32	45.39	431.17

In the VGSTSMC switching method, sliding surface, $s = \dot{e} + \rho_1 e$ and control signal, $u_1 = -(J/B_e)(-\ddot{q}_d + (1/J)(\tau_p - G) + u_2)$ are determined. Signals $u_2 = -\rho_2 \dot{e} + u_3$, $u_3 = -k_1(\theta, e)\varphi_1(s) - \int_0^t k_2(\theta, e)\varphi_2(s)d\theta$ and $\varphi_1(s) = |s|^{1/2}\text{sign}(s) + k_3 s$ and $\varphi_2(s) = (1/2)\text{sign}(s) + (3/2)k_3|s|^{1/2}\text{sign}(s) + k_3^2 s$ are considered. The switching signal is $\varepsilon \in \{-1, 1\}$, which determines the control signal with motor actuator dynamics, $B_1 = k_m$ or with

$B_{-1} = \left(c_1 e^{\frac{-(\phi - c_2)^2}{2c_3}} \right) \left(c_4 \left[1 + \tanh \left(c_5 \dot{\phi} + \frac{1}{c_4} \right) \right] \right)$, which is the FES dynamics actuator, to be applied to the system. According to the switching law, in the region $F = \{ \mu \vee \mu \in [\mu_{min}, \mu_{max}] \}$, the switch is made from FES to the motor. The values of the constant parameters of the system dynamics and controllers are shown in Table 7.

Table 7. VGSTSMC method parameters.

Parameter	Value	Parameter	Value
c_1	248.7	ρ_1	1
c_2	1.38	ρ_2	30
c_3	0.82	k_3	5
c_4	0.587	k_m	1
c_5	1.38		

The functions $k_1(\theta, e)k_2(\theta, e) = 1$, according to [8], are considered as a constant function. The fatigue region is $[\mu_{min}, \mu_{th}] = [0, 0.93]$.

Figure 14 shows the knee joint regulation simulation results. The transient state error for the VGSTSMC method and the oscillations of the hybrid PID method in the steady state are magnified in the diagram of each method. Oscillations are equivalent to the continuous movements of the knee, which, although it does not destroy regulation, is not desirable for practical application.

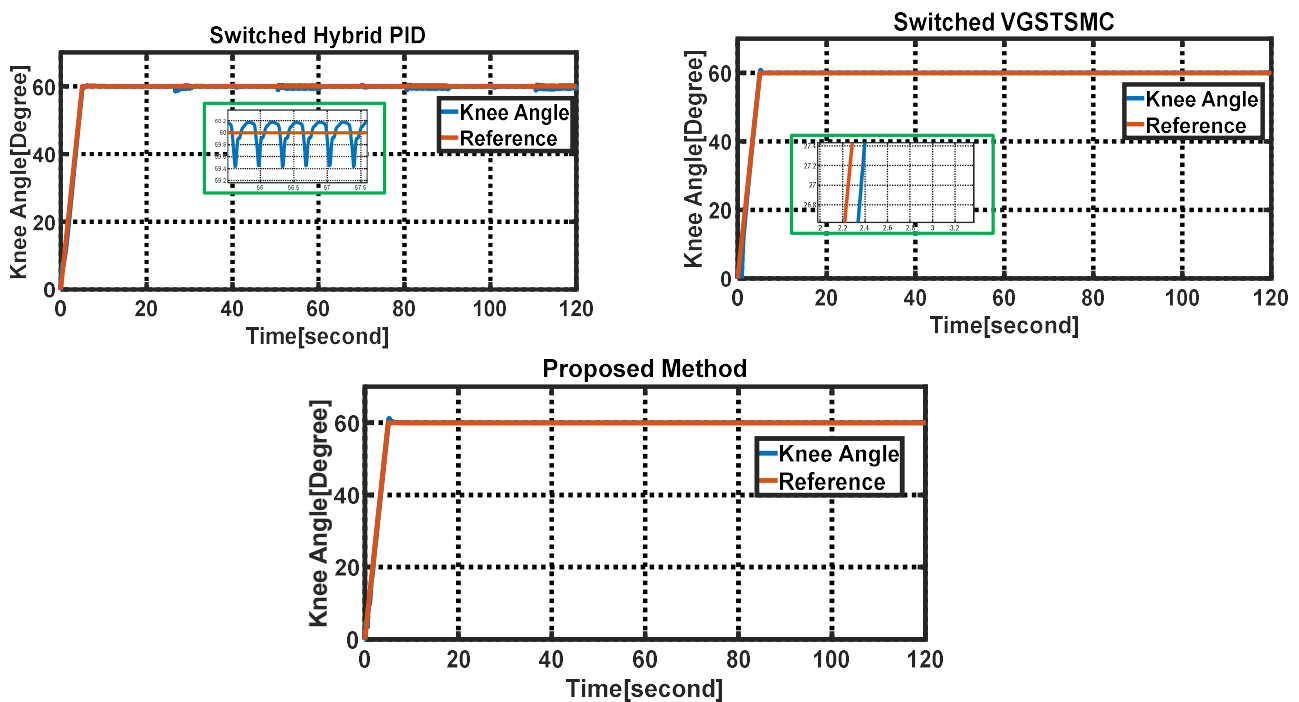


Figure 14. The knee joint regulation by PID hybrid switching (top-left), VGSTSMC switching (top-right), and the proposed method (bottom).

The proposed method, with more accurate reference path tracking and a lack of fluctuations, shows a more reliable performance for practical implementation.

The knee joint error for each method is shown in Figure 15. In the hybrid PID method, oscillations are observed in the steady state. In the transition state, the VGSTSMC switching method has a higher error than the proposed method due to the time it takes to place the system dynamics on the sliding surface.

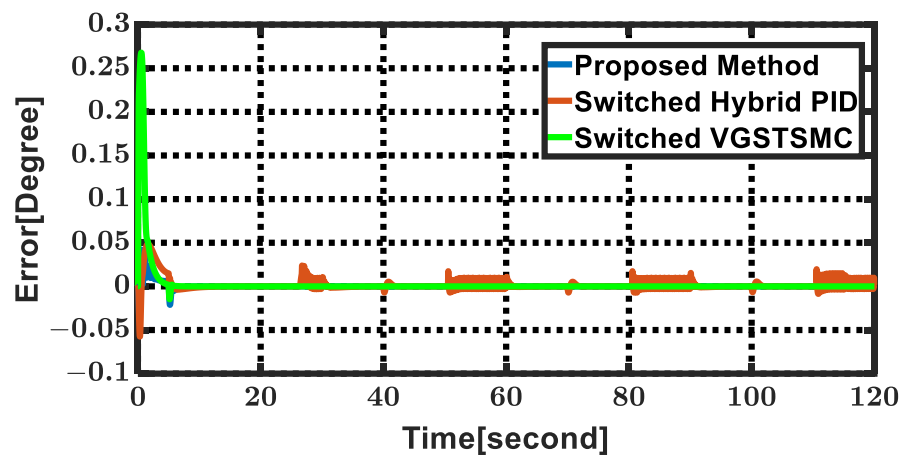


Figure 15. Knee joint angle error.

The RMS error, the RMS error in the transition state, and the RMS error in the steady state are recorded in Table 8. The proposed method, the hybrid PID switching method, and the VGSTSMC switching method regulated the joint successfully; the proposed method had less error than the other two methods. The proposed method with more accurate reference path tracking and lack of fluctuation showed a more reliable performance for practical implementation.

Table 8. RMS errors.

Control Methods	RMS Error [Degree]	Transient RMS Error [Degree]	Steady RMS Error [Degree]
Proposed Method	0.19	0.68	6.27×10^{-5}
Switched Hybrid PID	0.16	1.33	0.16
Switched VGSTSMC	1.26	4.38	2.25×10^{-4}

The muscle fatigue diagram of the investigated methods is shown in Figure 16. The proposed method and two switching-based methods showed an acceptable performance dealing with muscle fatigue and set the muscle fatigue in the neighborhood of the threshold value, $\mu_{th} = 0.93$. In the hybrid PID method, the switch from FES to the motor occurred at a greater distance than the fatigue threshold, and the muscle was more fatigued than in other methods.

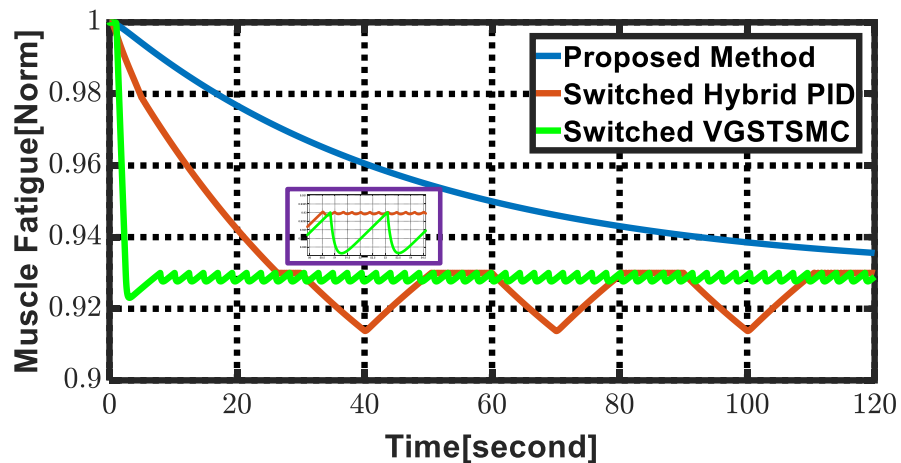


Figure 16. Muscle fatigue diagram.

Figure 17 shows the muscle activation diagrams. In the VGSTSMC switching method, the highest amount of muscle activation was required, and in the hybrid PID method, many changes in the muscle activation were observed; this is not desirable and presents a challenge for the practical implementation of the method.

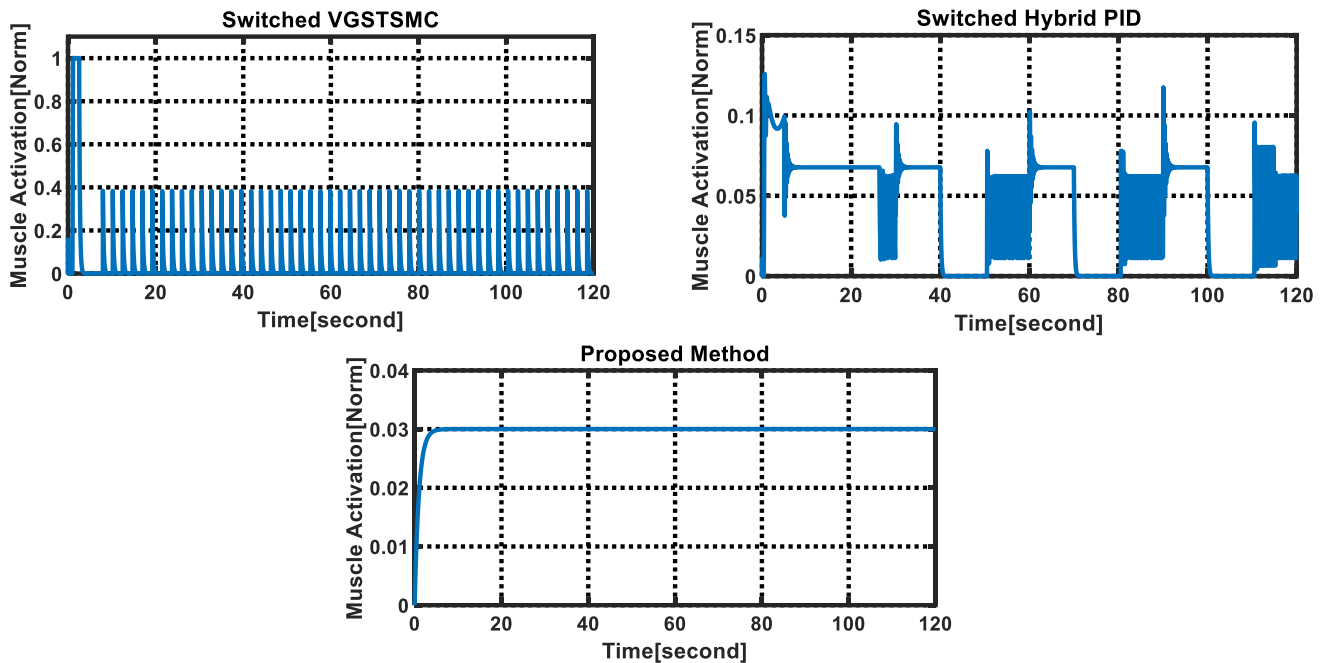


Figure 17. Muscle activation diagrams for VGSTSMC switching (top-left), hybrid PID switching (top-right), and the proposed method (bottom).

The chart of muscle fatigue variance for the proposed method and two switching-based methods is shown in Figure 18. In the VGSTSMC switching method, muscle fatigue was set with the lowest variance for the fatigue threshold value, which required fast switches in the system. In the practical application of fast switches, this caused the depreciation of actuators and controllers and challenged the implementation of method due to the highspeed switching.

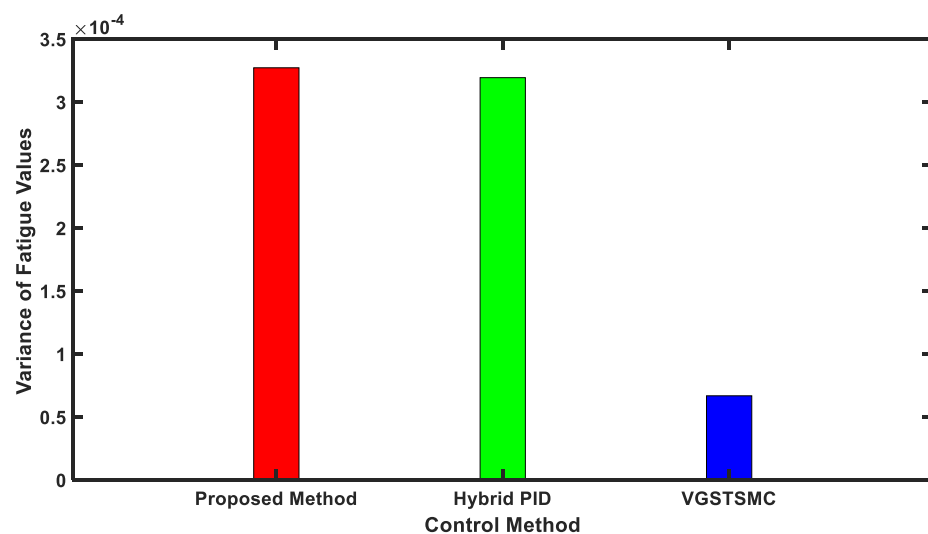


Figure 18. The muscle fatigue variance chart.

To evaluate the proposed method, PID hybrid switching method, and VGSTSMC switching method in muscle fatigue control, the average values of muscle fatigue, the

variance of muscle fatigue, minimum value of μ , maximum value of α_{ke} , and fatigue time were compared with each other; these values are shown in Table 9. Fatigue time was the first instant when the muscle fatigue was less than or equal to the muscle fatigue threshold $\mu_{th} = 0.93$. The fatigue instant of the VGSTSMC method was less than the other two methods, which indicates faster muscle fatigue with this method.

Table 9. Muscle fatigue and muscle activation indices.

Control Methods	Muscle Fatigue Values Mean	Muscle Fatigue Values Variance	Minimum of μ	Maximum of α_{ke}	Fatigue Instant [Second]
Proposed Method	0.95	3.27×10^{-4}	0.93	0.03	$t > 120$
Switched Hybrid PID	0.93	3.19×10^{-4}	0.91	0.12	26.35
Switched VGSTSMC	0.92	6.68×10^{-5}	0.92	1	2.55

The proposed method had the best average muscle fatigue compared with the other methods. In the proposed method, the fatigue instant did not occur during the simulation, there was no need for switching, and the lowest amount of muscle fatigue was obtained in this method. In the proposed method, without interrupting the stimulation, the amount of muscle activation was set at the desired value and muscle fatigue was regulated—the main advantage of the proposed method.

5. Discussion

5.1. Proposed Method Assessment

In this study, the regulation of muscle activation, muscle fatigue, and joint angle in the knee hybrid exoskeleton is provided by designing two controllers for muscle and joints in an innovative cooperative structure. Based on the simulation results, the proposed method can be clinically implemented to rehabilitate knee extension movement by stimulating the quadricep muscles through the hybrid knee exoskeleton. The innovations and contributions of the proposed method can be expressed as follows.

Innovations: (1) The control structure is designed for the knee hybrid exoskeleton in which the joint and muscle are controlled separately. (2) The estimation rule is designed to determine the time-varying parameter in the dynamic model of muscle activation. (3) The innovative adaptive controller is designed to regulate muscle activation. The control law consists of the state feedback and output error terms. The adaptation law is created by estimating the muscle activation time parameter. (4) The optimal PI controller is designed to control the knee joint; separate control of muscle activation causes disturbance to the joint, the PI controller, making the joint robust against that disturbance. (5) The relationship between muscle fatigue and muscle activation is computed, then muscle fatigue is regulated by muscle activation control.

Contributions: (1) This study presents the control method for the knee hybrid exoskeleton that automatically regulates knee joint angle and muscle activation. (2) In this study, the regulation of muscle fatigue is presented as the solution to increasing muscle fatigue due to electrical stimulation. Muscle fatigue regulation avoids stopping FES in knee rehabilitation due to increased muscle fatigue. (3) The muscle activation Hill-type-based model is improved by replacing the time-varying parameter instead of the muscle activation time constant and this replacement eliminates the pretest stage to estimate the parameter of the muscle activation model [35]. (4) The muscle control method's stability is proven by Lyapunov analysis, and the error bound of muscle activation is determined.

5.2. Proposed Method Advantages in Comparison with Other Methods

In iterative learning controller (ILC) methods, the joint tracking error in initial iterations is significant [11,13,17]. The time required to learn the controller is time consuming, which can hurt the patient psychologically. Part of the treatment session time is spent on controller learning, and treatment effectiveness is reduced [44]. A large volume of data are not readily available for patients who have undergone rehabilitation using a hybrid

knee exoskeleton. The lack of device testing results and the legal restrictions on access to personal health data make it challenging to collect this data. Therefore, training neural networks for model identification or controller design and validating the neural network methods in hybrid exoskeletons is challenging. The proposed method can control the knee joint hybrid exoskeleton without requiring a large amount of data and without iteration errors, which is the advantage of the proposed method over learning-based methods.

Methods based on model predictive and hierarchical control must solve complex optimization problems. Utilizing a hybrid exoskeleton faces a severe challenge in the laboratory implementation of these calculations. The delay in the experimental applications challenges the efficiency of lengthy and time-consuming calculations. The need for high-level hardware to quickly perform complex calculations is expensive and increases the cost of hybrid exoskeleton rehabilitation. The proposed method can be implemented on standard microcontrollers and average computers without complex and time-consuming calculations, which is the advantage of the proposed method over model predictive and hierarchical controllers.

The numerical evaluation of the proposed method, with other hybrid exoskeleton control methods, is completed by comparing the results of this study with the results of nonlinear model predictive control (NMPC) [20], linearized model predictive control (Linearized MPC) [20], shared iterative learning control (Shared ILC) [17], and Adaptive Low dimension control (ALDC) [45], based on Table 10. The evaluation is performed on the two main hybrid exoskeleton performance indexes: RMS error of angle and muscle fatigue. The improvement percentage for RMS error of angle and the muscle fatigue converged value by the proposed method of this study is determined compared with other methods. Compared with the other methods presented in Table 10, the main advantage of the proposed method is that muscle fatigue can be regulated at any desired value; in Table 10, the desired fatigue is valued as $\mu = 0.95$. In all cases in Table 10, the extension movement of the knee joint is considered.

Table 10. Comparison of the RMS error of angle and muscle fatigue.

Control Method	RMS Error of Angle [Degree]	Converged Fatigue Value [Norm]	RMS Error Improvement	Muscle Fatigue Improvement
Proposed Method	0.19	0.95	-	-
NMPC	0.52	0.8	63%	18.75%
Linearized MPC	2.23	0.7	91.47%	35.71%
Shared ILC	1.91	Not reported	90.05%	-
ALDC	2.82	0.75	93.26%	26.66%

Compared with the NMPC, Linearized MPC, Shared ILC, and ALDC methods, the proposed method resulted in 63%, 91.47%, 90.05%, and 93.26% improvement in angle RMS error, respectively. In addition, the proposed method led to 18.75%, 35.71%, and 26.66% improvements in muscle fatigue compared with NMPC, Linearized MPC, and ALDC, respectively. It is imperative to clarify that despite the requirement for a clinical examination for the validation of the proposed approach, wherein factors such as the nature and extent of the patient's injury have a significant impact on the outcomes, this comparison served to validate the efficacy of the proposed control approach from a theoretical standpoint and to establish the significance of its clinical evaluation.

Regulating muscle fatigue at a desired reference is difficult in switching-based methods. In switching control methods, muscle fatigue is limited in a region, but fatigue also increases in a region. In addition, switching faces limitations such as chattering and actuator depreciation due to many switches, but the proposed method prevents chattering and ensures the safety of actuators. The simulation results of the proposed method and switching-based methods are discussed to further investigate the comparison of these methods.

The proposed method has a 99% improvement in the knee joint angle steady state error compared with the hybrid PID switching method. In the simulation results in Figure 15,

intermittent fluctuations in the joint angle are observed in a steady state when the FES is active for the hybrid PID switching method. These fluctuations increase the steady state error of the hybrid PID switching method. In the method proposed in this study, the oscillations are prevented by separating the muscle controller from the joint controller. Compared with the hybrid PID method, smooth knee joint regulation is an important advantage of the proposed method for clinical applications. The proposed method results in an 84% improvement in RMS error compared with the VGSTSMC switching method. The VGSTSMC switching method to reach the sliding surface has a significant error in the transient state. In the transient state, the proposed method smoothly passes the transient phase and performs better than the VGSTSMC switching method. The vital advantage of the proposed method in knee joint regulation is its smooth movement. The presence of intermittent oscillations, such as those observed in the hybrid PID switching method, is annoying for the patient in practical applications. In addition, overshooting to reach the sliding surface, as seen in the VGSTSMC switching method, is challenging for a patient with mobility disorders.

The most important feature of the proposed method is the regulation of muscle fatigue at a desired value. Switching methods are also used to keep muscle fatigue in a specific region and to prevent the decrease of μ from a threshold value of μ_{th} . The value $\mu_{th} = 0.93$ is considered the threshold value in the simulations. The hybrid PID switching method has not succeeded in preventing the decrease of μ from the threshold value, and by decreasing the value of μ , the switch from FES to the motor occurs at $\mu = 0.91$. Although the difference in the μ value that the FES switches to the motor does not have a significant difference with the threshold value, in cases where the muscle fatigue threshold is defined at the border of complete fatigue, it can be challenging to perform the switch at a value lower than μ_{min} .

In this study, the average and variance of μ were used for the switching analysis, based on Table 9, without counting the switch numbers. A low variance for a mean value close to the fatigue threshold indicates more switches. The VGSTSMC switching method maintained the value of μ at the fatigue threshold, but the number of switches was enormous. In practice, implementing these switch numbers faces challenges due to limitations such as electromechanical delay and depreciation of actuators. The proposed method maintained the μ value higher than the fatigue threshold throughout the simulation. In the VGSTSMC switching method, muscle fatigue increased very quickly, but in the proposed method, the fatigue increased gently and did not decrease from the threshold value. In the hybrid PID switching and VGSTSMC switching methods, when μ was less than the threshold value, FES was disabled, and $\alpha_{ke} = 0$, according to Figure 17. Muscle activation due to electrical stimulation is one of the main goals of rehabilitation. In Figure 17, it can be seen that by using the proposed method, the muscle activation was regulated at a desired value. In addition, by regulating muscle fatigue, there was no need to deactivate the FES, and the primary goal of rehabilitation was achieved.

5.3. Proposed Method Advantages in Clinical Implementation

The proposed method has a significant advantage over other hybrid exoskeleton control methods. In other methods, to estimate the time constant of muscle activation, it is necessary to perform a pre-experiment stage [19,21]. This stage prolongs the rehabilitation time and can cause physical and mental fatigue in the patient [37]. The proposed method eliminates the pre-experiment stage for estimating the muscle activation time constant. Therefore, the practical use of the hybrid knee exoskeleton becomes more convenient. Adaptive controller design utilizing the model parameter time-varying estimation as an adaptation law increases the possibility of a patient's personalized rehabilitation.

Although the pre-experiment stage is still needed to determine the recovery time and fatigue time parameters, this stage can be eliminated by time-varying estimating these parameters. Due to muscle activation's controllability and the importance of muscle activation in determining muscle fatigue, this article focuses on muscle activation control.

Muscle fatigue desired value regulation and muscle activation error bound prediction can help therapists design a more accurate plan for the patient's rehabilitation. The therapist can plan the number of sessions, the duration of each session, and the intensity of the patient's exercises by simulating the proposed method before rehabilitation. In addition, the therapist can mix the knee hybrid exoskeleton, which the proposed method controls, along with other rehabilitation methods in therapy processes [46].

5.4. Limitations

As a result of the presence of delay in natural systems, the effect of delay on the proposed method is a limitation in its implementation [12]. This study did not consider the disturbance's effects on the system's performance [47]. The existence of disturbances, especially in biological systems, is another challenge to the proposed method's implementation. The expert supervision necessity for practical testing is another limitation in the proposed method implementation. Various factors, such as mental factors, affect muscle fatigue; these factors differ from one individual to another depending on the rehabilitation conditions [28]. The unmodeled muscle fatigue factors are another limitation of the proposed method's implementation [48,49]. Based on the simulation results, the proposed method can be implemented, but for more accurate evaluation, it is necessary to test it in a laboratory and on sufficient subjects.

6. Conclusions

In this study, the method of regulating muscle fatigue by controlling muscle activation was presented to overcome the challenge of muscle fatigue in the knee hybrid exoskeleton. An innovative control structure was used to control the joint and muscle separately. The PI controller was designed to regulate the joint angle with an optimal control method. A new adaptive controller was designed to control the muscle using an indirect adaptive method. The muscle activation time parameter was estimated in the muscle model and controller. The relationship between muscle fatigue and muscle activation was calculated in fatigue regulation for the first time. The UUB of muscle activation error was proven using Lyapunov analysis. The proposed method simulation was performed, and the controllers' performance results were evaluated for regulating muscle fatigue and joint angle regulation, which determined the control objective and the system's performance. The obtained results showed significant success in providing the control objective and improving the system performance, and for the first time, muscle fatigue was regulated in the hybrid exoskeleton. The proposed method was compared with MPC-based and switching methods, and the results showed significantly improved muscle fatigue indexes and RMS joint angle error. Not considering the delay and disturbance effect and the need for laboratory implementation under the therapist's supervision to evaluate the method are limitations of the proposed method. More accurately evaluating the proposed method requires clinical testing with sufficient subjects. However, the simulation results confirm the possibility of practical implementation of the proposed method and its capability for personalized rehabilitation.

Future Works

The proposed method, implementation in the laboratory and on human subjects is suggested for future studies. Furthermore, the proposed method can be investigated in future studies using online real-time implementation. The online real-time method determines muscle fatigue [50], so a controller design that regulates muscle activation and muscle fatigue without a muscle model is considered. Dynamic models and learning-based methods are combined to control exoskeletons [51]. Hybrid exoskeleton control by combining classical dynamic equations and learning methods, such as reinforcement learning [52], needs to be considered for future study to deal with model uncertainty and delay.

Author Contributions: conceptualization, S.G. and H.K.; data curation, S.G. and H.K.; formal analysis, S.G., R.K.M. and H.K.; investigation, S.G.; methodology, N.P. and H.K.; project administration, N.P. and R.K.M.; resources: S.G. and H.K.; software: S.G.; supervision: N.P. and R.K.M.; validation, R.K.M. and H.K.; visualization: S.G. and R.K.M.; writing—original draft: S.G.; writing—review and editing: R.K.M. All authors have read and agreed to the published version of the manuscript.

Funding: This research received no external funding.

Data Availability Statement: Not applicable.

Conflicts of Interest: The authors declare no conflict of interest.

References

1. Anaya, F.; Thangavel, P.; Yu, H. Hybrid FES–robotic gait rehabilitation technologies: A review on mechanical design, actuation, and control strategies. *Int. J. Intell. Robot. Appl.* **2018**, *2*, 1–28. [[CrossRef](#)]
2. Cimolato, A.; Driessen, J.J.; Mattos, L.S.; De Momi, E.; Laffranchi, M.; De Michieli, L. EMG-driven control in lower limb prostheses: A topic-based systematic review. *J. NeuroEngineering Rehabil.* **2022**, *19*, 43. [[CrossRef](#)] [[PubMed](#)]
3. Voloshina, A.S.; Collins, S.H. Lower limb active prosthetic systems—Overview. *Wearable Robot.* **2020**, 469–486. [[CrossRef](#)]
4. Dunkelberger, N.; Scheerer, E.M.; O'Malley, M.K. A review of methods for achieving upper limb movement following spinal cord injury through hybrid muscle stimulation and robotic assistance. *J. Exp. Neurol.* **2020**, *328*, 113274. [[CrossRef](#)] [[PubMed](#)]
5. Gil-Castillo, J.; Alnajjar, F.; Koutsou, A.; Torricelli, D.; Moreno, J.C. Advances in neuroprosthetic management of foot drop: A review. *J. Neuroeng. Rehabil.* **2020**, *17*, 46. [[CrossRef](#)]
6. Masengo, G.; Zhang, X.; Dong, R.; Alhassan, A.B.; Hamza, K.; Mudaheranwa, E. Lower limb exoskeleton robot and its cooperative control: A review, trends, and challenges for future research. *Front. Neurobot.* **2023**, *16*, 913748. [[CrossRef](#)]
7. Sheng, Z.; Iyer, A.; Sun, Z.; Kim, K.; Sharma, N. A hybrid knee exoskeleton using real-time ultrasound-based muscle fatigue assessment. *IEEE/ASME Trans. Mechatron.* **2022**, *27*, 1854–1862. [[CrossRef](#)]
8. Kirsch, N.; Alibeji, N.; Dicianno, B.E.; Sharma, N. Switching control of FES and motor assist for muscle fatigue compensation. In Proceedings of the 2016 American Control Conference (ACC), Boston, MA, USA, 6–8 July 2016; IEEE: Washington, DC, USA, 2016; Volume 16193830. [[CrossRef](#)]
9. Molazadeh, V.; Sheng, Z.; Sharma, N. A Within-Stride Switching Controller for Walking with Virtual Constraints: Application to a Hybrid Neuroprosthesis. In Proceedings of the 2018 Annual American Control Conference (ACC), Milwaukee, WI, USA, 27–29 June 2018; IEEE: Washington, DC, USA, 2018; Volume 18008171, pp. 5286–5291.
10. Sheng, Z.; Molazadeh, V.; Sharma, N. Hybrid dynamical system model and robust control of a hybrid neuroprosthesis under fatigue based switching. In Proceedings of the 2018 Annual American Control Conference (ACC), Milwaukee, WI, USA, 27–29 June 2018; IEEE: Washington, DC, USA, 2018; Volume 18008786, pp. 1446–1451. [[CrossRef](#)]
11. Molazadeh, V.; Sheng, Z.; Bao, X.; Sharma, N. A robust iterative learning switching controller for following virtual constraints: Application to a hybrid neuroprosthesis. *IFAC-PapersOnLine* **2019**, *51*, 28–33. [[CrossRef](#)]
12. Sheng, Z.; Sun, Z.; Molazadeh, V.; Sharma, N. Switched control of an N-degree-of-freedom input delayed wearable robotic system. *Automatica* **2021**, *125*, 109455. [[CrossRef](#)]
13. Molazadeh, V.; Zhang, Q.; Bao, X.; Sharma, N. An iterative learning controller for a switched cooperative allocation strategy during sit-to-stand tasks with a hybrid exoskeleton. *IEEE Trans. Control Syst. Technol.* **2021**, *30*, 1021–1036. [[CrossRef](#)]
14. Ghajari, S.; Moghaddam, R.K.; Kobravi, H.R.; Pariz, N. Knee Joint Movement Control Using Hybrid Neuro-prosthesis Based on Persistent D-well Time Allocation Strategy with Muscle Fatigue Overcoming: Simulation Approach. *JRRS* **2022**, *18*, 12–23.
15. Zhang, D.; Yong, R.; Gui, K.; Jia, J.; Wendong, X. Cooperative Control for A Hybrid Rehabilitation System Combining FES and Robotic Exoskeleton. *Front. Neurosci.* **2017**, *11*, 725. [[CrossRef](#)]
16. Bao, X.; Molazadeh, V.; Dodson, A.; Dicianno, B.E.; Sharma, N. Using person-specific muscle fatigue characteristics to optimally allocate control in a hybrid exoskeleton—Preliminary results. *IEEE Trans. Med. Robot. Bionics* **2020**, *2*, 226–235. [[CrossRef](#)] [[PubMed](#)]
17. Molazadeh, V.; Zhang, Q.; Bao, X.; Dicianno, B.E.; Sharma, N. Shared control of a powered exoskeleton and functional electrical stimulation using iterative learning. *Front. Robot. AI* **2021**, *8*, 711388. [[CrossRef](#)]
18. Kirsch, N.; Alibeji, N.; Sharma, N. Model predictive control-based dynamic control allocation in a hybrid neuroprosthesis. In Proceedings of the ASME 2014 Dynamic Systems and Control Conference, San Antonio, TX, USA, 22–24 October 2014; American Society of Mechanical Engineers: Washington, DC, USA, 2014; Volume 46209, p. V003T43A003. [[CrossRef](#)]
19. Kirsch, N.; Bao, X.; Alibeji, N.; Dicianno, B.; Sharma, N. Model-based dynamic control allocation in a hybrid neuroprosthesis. *IEEE Trans. Neural Syst. Rehabil. Eng.* **2017**, *26*, 224–232. [[CrossRef](#)] [[PubMed](#)]
20. Bao, X.; Kirsch, N.; Dodson, A.; Sharma, N. Model Predictive Control of a Feedback Linearized Hybrid Neuroprosthetic System with a Barrier Penalty. *ASME. J.* **2019**, *14*, 101009. [[CrossRef](#)]

21. Bao, X.; Sheng, Z.; Dicianno, B.E.; Sharma, N. A Tube-Based Model Predictive Control Method to Regulate a Knee Joint with FES and Electric Motor Assist. *IEEE Trans. Control Syst. Technol.* **2020**, *9*, 2180–2191. [[CrossRef](#)]
22. Bao, X.; Mao, Z.H.; Munro, P.; Sun, Z.; Sharma, N. Sub-optimally solving actuator redundancy in a hybrid neuroprosthetic system with a multi-layer neural network structure. *Int. J. Intell. Robot. Appl.* **2019**, *3*, 298–313. [[CrossRef](#)] [[PubMed](#)]
23. Tu, X.; Li, J.; Li, J.; Su, C.; Zhang, S.; Li, H.; Cao, J.; He, J. Model-based hybrid cooperative control of hip-knee exoskeleton and FES induced ankle muscles for gait rehabilitation. *Intern. J. Pattern Recognit. Artif. Intell.* **2017**, *31*, 1759019. [[CrossRef](#)]
24. Alibeji, N.; Molazadeh, V.; Dicianno, B.E.; Sharma, N. A control scheme that uses dynamic postural synergies to coordinate a hybrid walking neuroprosthesis: Theory and experiments. *Front. Neurosci.* **2018**, *12*, 159. [[CrossRef](#)]
25. Del-Ama, A.J.; Gil-Agudo, Á.; Pons, J.L.; Moreno, J.C. Hybrid FES-robot cooperative control of ambulatory gait rehabilitation exoskeleton. *J. Neuroeng. Rehabil.* **2014**, *11*, 27. [[CrossRef](#)] [[PubMed](#)]
26. Del-Ama, A.J.; Gil-Agudo, Á.; Pons, J.L.; Moreno, J.C. Characterization of a Dual PID-ILC FES Controller for FES-Robot Control of Swing Phase of Walking. In *Replace, Repair, Restore, Relieve—Bridging Clinical and Engineering Solutions in Neurorehabilitation*, 1st ed.; Jensen, W., Andersen, O., Pons, J., Moreno, J.C., Eds.; Springer: Cham, Switzerland, 2014; Volume 7, pp. 341–349. [[CrossRef](#)]
27. De Sousa, A.C.; Freire, J.P.; Bo, A.P. Integrating hip exosuit and FES for lower limb rehabilitation in a simulation environment. *IFAC-PapersOnLine* **2019**, *51*, 302–307. [[CrossRef](#)]
28. Wan, J.J.; Qin, Z.; Wang, P.Y.; Sun, Y.; Liu, X. Muscle fatigue: General understanding and treatment. *Exp. Mol. Med.* **2017**, *49*, e384. [[CrossRef](#)] [[PubMed](#)]
29. Bulea, T.C.; Sharma, N.; Sikdar, S.; Su, H. Next generation user-adaptive wearable robots. *Front. Robot. AI* **2022**, *9*, 920655. [[CrossRef](#)] [[PubMed](#)]
30. Müller, P.; Del Ama, A.J.; Moreno, J.C.; Schauer, T. Adaptive multichannel FES neuroprosthesis with learning control and automatic gait assessment. *J. Neuroeng. Rehabil.* **2020**, *17*, 36. [[CrossRef](#)]
31. Popovic, D.; Stein, R.B.; Oguztoreli, M.N.; Lebedowska, M.; Jonic, S. Optimal control of walking with functional electrical stimulation: A computer simulation study. *IEEE Trans. Neural Syst. Rehabil. Eng.* **1999**, *7*, 69–79. [[CrossRef](#)]
32. Kirsch, N.; Alibeji, N.; Sharma, N. Nonlinear model predictive control of FES. *Control Eng. Pract.* **2017**, *58*, 319–331. [[CrossRef](#)]
33. Ober-Blöbaum, S.; Offen, C. Variational learning of Euler–Lagrange dynamics from data. *J. Comput. Appl. Math.* **2023**, *421*, 114780. [[CrossRef](#)]
34. Riener, R.; Quintern, J.; Schmidt, G. Biomechanical model of the human knee evaluated by neuromuscular stimulation. *J. Biomech.* **1996**, *29*, 1157–1167. [[CrossRef](#)]
35. Veltink, P.H.; Chizeck, H.J.; Crago, P.E.; El-Bialy, A. Nonlinear joint angle control for artificially stimulated muscle. *IEEE Trans. Biomed. Eng.* **1992**, *39*, 368–380. [[CrossRef](#)]
36. Carsten, B.; Siedler, K. Adaptive PID-tracking Control of Muscle-like Actuated Compliant Robotic Systems with Input Constraints. *Appl. Math. Model.* **2019**, *67*, 9–21. [[CrossRef](#)]
37. Alif, T.; Bhasin, S.; Garg, K.; Joshi, D. An Enhanced Model Free Adaptive Control Approach for Functional Electrical Stimulation Assisted Knee Joint Regulation and Control. *IEEE Trans. Neural Syst. Rehabilitation Eng.* **2023**, *31*, 1584–1593. [[CrossRef](#)] [[PubMed](#)]
38. Khalil, H. *Nonlinear Systems*; Pearson: London, UK, 2003; pp. 400–401.
39. Astrom, K.J.; Wittenmark, B. *Adaptive Control*; Dover Publications Inc.: Boston, MA, USA, 2008; pp. 100–105.
40. Xu, J.X. A survey on iterative learning control for nonlinear systems. *Int. J. Control* **2011**, *84*, 1275–1294. [[CrossRef](#)]
41. Ding, Z. *Nonlinear and Adaptive Control Systems*; The Institution of Engineering and Technology: London, UK, 2013; pp. 150–152.
42. Baek, J.; Jin, M.; Han, S. A new adaptive sliding-mode control scheme for application to robot manipulators. *IEEE Trans. Ind. Electron.* **2016**, *63*, 3628–3637. [[CrossRef](#)]
43. Nunes, W.R.; Alves, U.N.; Sanches, M.A.; Teixeira, M.C.; De Carvalho, A.A. Electrically Stimulated Lower Limb using a Takagi-Sugeno Fuzzy Model and Robust Switched Controller Subject to Actuator Saturation and Fault under Nonideal Conditions. *Int. J. Fuzzy Syst.* **2022**, *24*, 57–72. [[CrossRef](#)]
44. Sa-e, S.; Freeman, C.T.; Yang, K. Iterative learning control of FES in the presence of voluntary user effort. *Control Eng. Pract.* **2020**, *96*, 104303. [[CrossRef](#)]
45. Alibeji, N.; Kirsch, N.; Sharma, N. An adaptive low-dimensional control to compensate for actuator redundancy and FES-induced muscle fatigue in a hybrid neuroprosthesis. *Control Eng. Pract.* **2017**, *59*, 204–219. [[CrossRef](#)]
46. Michelle, H.; Cameron, M. *Physical Agents in Rehabilitation: An Evidence-Based Approach to Practice*; Elsevier: Berkeley, CA, USA; Saunders: Philadelphia, PA, USA, 2017; pp. 77–84.
47. Rakhtala, S.M. Adaptive gain super twisting algorithm to control a knee exoskeleton disturbed by unknown bounds. *Int. J. Dyn. Control* **2021**, *9*, 711–726. [[CrossRef](#)]
48. Wang, Y.; Lu, C.; Zhang, M.; Wu, J.; Tang, Z. Research on the Recognition of Various Muscle Fatigue States in Resistance Strength Training. *Healthcare* **2022**, *10*, 2292. [[CrossRef](#)]
49. Frey-Law, L.A.; Schaffer, M.; Urban, F.K. Muscle fatigue modelling: Solving for fatigue and recovery parameter values using fewer maximum effort assessments. *Int. J. Ind. Ergon.* **2021**, *82*, 103104. [[CrossRef](#)]
50. Zhang, Q.; Iyer, A.; Lambeth, K.; Kim, K.; Sharma, N. Ultrasound echogenicity as an indicator of muscle fatigue during functional electrical stimulation. *Sensors* **2022**, *22*, 335. [[CrossRef](#)] [[PubMed](#)]

51. Tran, H.T.; Tan, L.N.; Han, S.H. Model-Learning-Based Partitioned Control of a Human-Powered Augmentation Lower Exoskeleton. *J. Electr. Eng. Technol.* **2022**, *17*, 533–550. [[CrossRef](#)]
52. Luo, S.; Androwis, G.; Adamovich, S.; Su, H.; Nunez, E.; Zhou, X. Reinforcement learning and control of a lower extremity exoskeleton for squat assistance. *Front. Robot. AI* **2021**, *8*, 702845. [[CrossRef](#)] [[PubMed](#)]

Disclaimer/Publisher’s Note: The statements, opinions and data contained in all publications are solely those of the individual author(s) and contributor(s) and not of MDPI and/or the editor(s). MDPI and/or the editor(s) disclaim responsibility for any injury to people or property resulting from any ideas, methods, instructions or products referred to in the content.